CHALMERS
UNIVERSITY OF TECHNOLOGY

A comparison of elastic mooring systems for floating wave energy converters

Master's thesis in the International Master's Programme in Naval Architecture and Ocean Engineering

HO-ANN CHEN

DEPARTMENT OF MECHANICS AND MARITIME SCIENCES

CHALMERS UNIVERSITY OF TECHNOLOGY

Gothenburg, Sweden 2020

www.chalmers.se

MASTER'S THESIS IN THE INTERNATIONAL MASTER'S PROGRAMME
NAVAL ARCHITECTURE AND OCEAN ENGINEERING

A Comparison of Elastic Mooring Systems for Floating Wave Energy Converters

HO-ANN CHEN

Department of Mechanics and Maritime Sciences

Division of Marine Technology

CHALMERS UNIVERSITY OF TECHNOLOGY

Göteborg, Sweden 2020

A Comparison of Elastic Mooring Systems for Floating Wave Energy Converters

HO-ANN CHEN

Master's Thesis 2020:41

Department of Mechanics and Maritime Sciences

Division of Marine Technology

Chalmers University of Technology

SE-412 96 Göteborg
Sweden
Telephone: + 46 (0)31-772 1000

Printed by Chalmers Reproservice

Göteborg, Sweden 2020

A Comparison of Elastic Mooring Systems for Floating Wave Energy Converters

Master's thesis in the International Master's Programme Naval Architecture and Ocean Engineering

HO-ANN CHEN

Department of Mechanics and Maritime Sciences
Division of Marine Technology
Chalmers University of Technology

Abstract

Wave energy is a widespread and abundant source of renewable energy, yet the technology of harnessing energy from waves is still in the pre-commercial stage. One of the key challenges in the development of wave energy converters (WEC) technology is to ensure the long-term performance and reliability of the mooring system, which must be designed to survice under cyclic loading, not fail due to fatigue, at a commercially competitive cost. This thesis takes WaveEL, a heaving point-absorbing WEC developed by Waves4Power, as the reference case to investigate the performance of WEC systems with different elastic mooring systems in regards to fatigue life and power absorption. As the electricity production of the heaving point-absorber WEC relies on the cyclic heave motion of the WEC device, the long-term deployment of the WEC systems under irregular ocean loads poses high fatigue damage on the mooring lines. The snap loads that act on the mooring lines also decrease the mechanical life of the mooring system.

Studies have shown that by adding tether components to the mooring system, the fatigue life of the system can be increased, thus making the WEC systems more commercially feasible. A tether component is a mechanical system that reduces the responding force range and absorb the snap loads in mooring lines. It is this thesis' objective to develop numerical models to represent tether components, and to evaluate its impact on the WEC performance by integrating the elastic tether component into the mooring system. This thesis investigates two mooring configurations: a 3-leg mooring system with floating buoys between the WEC device and the anchor to decreases the stress loading on the mooring lines, and a 2-leg mooring system with a deeper design water depth so that the system can benefit from the elasticity of the mooring lines. Comparisons are made between the two original mooring configurations and the same mooring setup with the tether component implemented.

Coupled hydrodynamic-structural simulations are carried out with different mooring configurations under operational loads. The heave motions of the WEC device and the force response in the mooring lines under operation conditions are obtained from the simulation results and used to calculate the fatigue life of the mooring system and the absorbed power of the WEC system. It was found that the tether component greatly improves the fatigue life of the mooring system, whilst not negatively affecting the power absorption.

Key words: wave energy converter, mooring line, coupled simulation, elastic mooring tether, fatigue, power absorption, heaving point absorber.

Contents

Abstract I
Contents III
Preface V
Nomenclature VI
1 Introduction 1
1.1 Background and motivation of study 1
1.2 Objective and goals 4
1.3 Assumptions and delimitations 4
1.4 Outline of the thesis 6
2 Methodology 7
2.1 Mechanical constitutive model for tether component 8
2.2 Hydrodynamic and structure coupled simulations 12
2.3 Power absorption analysis 14
2.4 Fatigue damage analysis 14
2.5 Parametric sensitivity analysis 15
2.6 LCoE analysis 15
3 Numerical analysis 17
3.1 Modeling tether component for coupled simulations 17
3.2 Hydrodynamic-structural coupled simulations 18
3.2.1 Mooring designs 19
3.2.2 Simulation model set-up 20
3.2.3 Simulation matrix 23
3.2.4 Discretization of mooring lines 23
4 Results and discussion 27
4.1 Coupled hydrodynamic-structural simulation results 27
4.1.1 Decay test 27
4.1.2 Comparison of simulated wave elevation and WEC motion 28
4.1.3 Comparison of the simulated motion and force responses in the mooring lines 35
4.2 Fatigue analysis of mooring lines 37
4.3 Power absorption analysis 40
4.4 Parametric sensitivity analysis 42
4.5 Constitutive model for tether component 42
4.6 Cost analysis 44
4.6.1 LCoE analysis results 44
4.6.2 Cost recommendation for tether 45

5 Summary and conclusions 47
6 Future work 49
7 References 51
8 Appendix 55
8.1 Wave scatter diagram at Runde 55
8.2 Drawings and dimensions of WEC buoy and floaters 56
8.3 Static and dynamic calculation parameters in SIMA for base settings 57
8.4 Fatigue damage - irregular sea states 58

Preface

This thesis is part of the program's requirements for the master's degree at Chalmers University of Technology and has been carried out at the Division of Marine Technology, Department of Mechanics and Maritime Sciences, Chalmers University of Technology between January and June of 2020.

I would like to thank my supervisor and examiner for this thesis, Professor Jonas Ringsberg, for inviting me to this meaningful long-term research project. I would also like to thank him for his feedback and encouragement, which has guided me through this thesis project.

I would also like to thank my co-supervisor for this thesis project, Shun-Han Yang, for her guidance throughout these months, particularly her insights and expertise on this research topic, simulation, and modeling procedures. Her kind advice have helped me along the way. Not to mention the time and support she has given me throughout the process.

Special thanks goes to Lars Brandt and his colleagues at Seaflex. Their expertise and the discussions with them are helpful and very valuable for me.

Finally, I would like to thank my family and friends for their endless love and support. Thank you for always believing in me.

Göteborg, June 2020

HO-ANN CHEN

Nomenclature

List of acronyms

CoB	Center of buoyancy
CoG	Center of gravity
DoF	Degree of dreedom
FEM	Finite element method
FLS	Fatigue limit state
IEA	International Energy Agency
JONSWAP	Joint North Sea Wave Project
LCoE	Levelized cost of energy
ODE	Ordinary differential equation
PTO	Power take-off
RAO	Response amplitude operator
WEC	Wave energy converter

Latin notations

C	Damping coefficient [Ns^2/m^2]
Dir_{curr}	Direction of the incoming current [deg], defined as the angle of current relative to the x-axis of the coordinate system
Dir_{wave}	Direction of the incoming wave [deg], defined as the angle of the wave propagating direction relative to the x-axis of the coordinate system
Dir_{wind}	Direction of the incoming wind [deg], defined as the angle of the wind relative to the x-axis of the coordinate system
FD	Accumulated fatigue damage of the mooring line [-]
H_s	Significant wave height [m]
P	Strain velocity exponent [-]
$\bar{P}$	Time-averaged power absorption of the WEC [W]
t	Time [s]
T_p	Peak wave period [s]
V_{curr}	Current velocity [m/s]
V_{wind}	Wind velocity [m/s]

Greek notations

ε	Strain [-]
η	Damping ratio [Ns/m^2]
γ	Non-dimensional peak enhancement factor for JONSWAP spectrum [-]
σ	Axial stress [Pa]

List of symbols and unit abbreviations

deg	degrees
EUR	Euros
kg	kilograms
kW	kilowatt
m	meters
MWh	megawatts hour
N	newtons
s	seconds

1 Introduction

This chapter starts by presenting the background and motivation of the study. The goals and objectives are then derived from the motivation, where delimitations are drawn for this project. The introduction chapter ends with the outline of this thesis.

1.1 Background and motivation of study

Humankind is constantly looking for alternative solutions for energy demand. The United Nations defines clean and affordable energy as one of the sustainable development goals (UN, 2020), and being able to use renewable energy sources is an important part of achieving sustainability. Planet Earth is covered 70% by the ocean, making it very desirable to investigate the possibility of harnessing energy from the ocean. This thesis focuses on the development of wave energy technologies. Studies have shown that the energy stored in waves is more constant and predictable than solar energy or wind energy with a higher power density (Czech & Bauer, 2012), but the technology readiness is not as good as the other two. In addition to its high energy density, waves can travel a long distance with little energy loss (Drew et al., 2009). The European Commission has estimated that if 0.1% of the energy in the waves can be extracted, it could cover 5 times the global energy demand, annually (European Commission, 2016). It should be noted that due to different landscapes, shipping routes, operability, and other factors, not all areas around the globe is suitable or optimal for harnessing wave energy.

More than 250 companies are invested in the development of wave energy converter (WEC) systems, not to mention the numbers of devices and technologies that have been invented (EMEC, 2020), most of which are still in prototype stage and requires intensive testing to ensure the reliability of the systems. WEC systems typically incorporate 4 sub-components: a main structure to capture the mechanical energy in waves, a power take-off system to convert mechanical energy to electricity, a foundation or mooring system for station keeping and a control system to monitor the WEC system's performance (Falcao, 2010).

The terms used in this thesis should be clarified: when the "WEC system" is presented, it includes all components of the WEC system, including the WEC device, the mooring system, and power cables. "WEC device" only refers to the buoy where the heaving motion is transformed into electricity. As for the "mooring system", this refers to all components that serve the purpose of station-keeping, including the mooring lines, the connecting joints, the anchors, and the floaters if applicable.

WEC systems can be categorized by its location, its operation principles, its directional characteristics, and its power take-off (PTO) methods (Czech & Bauer, 2012). Location-wise, there are onshore, nearshore, and offshore sites. The main operation principles are:

- Oscillating water column, where an air camber is compressed when waves come into the water column, raising the water level and hence compressing the air.
- Overtopping device, where the device captures water from waves and generates electricity through the difference in potential energy.
- Wave-activated bodies, which the WEC device is excited by the wave force, and the motion of the WEC is translated into electricity.

The operation principle also depends on the system's directional characteristics: it can be a point absorber, perpendicular or parallel to the wave propagating direction. Linear generators, air turbines and hydraulic systems are the main PTO methods, which highly depends on the WEC system's operation principles and its directions.

Most of the WEC concepts, except for the onshore ones, require mooring systems for station-keeping. Though mooring systems have been developed over decades for different offshore structures, one fundamental design characteristics that should be noted for the WEC mooring systems, especially the point-absorbers, is that WEC devices are designed to resonate in the waves to maximize the energy harvest (Falcao, 2010). This characteristic differs greatly from mooring needs for the oil and gas industry, where the main purpose is station-keeping. This means that the development of conventional mooring for the oil and gas industry cannot be directly transferred to WEC usage. WEC devices are designed to respond strongly to wave forces, making the mooring system prone to large snap loads. Snap loads may reduce lifetime or cause immediate failure of the mooring systems. In extreme sea states (e.g. storms), the loading on the WEC system can be 100 times larger than average loading (Czech & Bauer, 2012), making it necessary to overdimension the design for the system's durability, which raises the design cost of the system.

The mooring systems for WEC systems constitute a difficult engineering challenge with two contradicting requirements: the need for station keeping and the need to allow large heaving motions of the WEC device. To allow large heaving motions, the mooring system must be elastic and gives freedom for cyclic extensions of the ropes. However, this introduces large cyclic stress responses in the mooring lines, which would likely cause fatigue damage on the mooring lines. Moreover, a report from the European Commission identified the need for increasing device reliability and survivability as one of the urgent technology challenges ocean energy development needs to tackle (TPOcean, 2017). If the mooring system fails, not only would it stop the electricity production, but it also poses a possible threat to the nearby WECs (if it is in a wave energy farm, where many devices lie in arrays), aquaculture and nearshore infrastructures.

Thus, this thesis aims to contribute to increasing the reliability of mooring systems for WEC systems, in particular, the floating point-absorbers. By making the mooring system's mechanical life at least as long as the designed service life, it may help make the WEC systems commercially competitive and more feasible in the long term.

The review done by Falcao in 2010 highlights that floating WEC concepts tend to be more complex than nearshore and onshore concepts (Falcao, 2010). For typical

machinery that undertakes a large amount of cyclic loadings, it is common practice to change the component periodically to ensure safety and reliability. However, maintaining floating WEC systems tends to be troublesome as WEC systems are offshore and do not have a static platform to perform maintenance on. Hence, investors and WEC operators tend to prefer systems with fewer components, for that the less complex the system is, the easier it is to maintain, and the less chances of entanglement (Rinaldi et al., 2016).

There is also financial reasoning for the need of developing an alternative mooring system. Yang et al. (2018b) proposed a mooring setup that can successfully increase the reliability of the mooring system by adding submerged floaters mid mooring line, between the WEC device and the anchor, see Fig.1-2. However, this increases the horizontal area that is needed for each installation. For the companies investing in WEC systems, the installation cost is determined by the mooring footprint. The mooring footprint is the horizontal area taken up by the mooring lines, where fishery and transportation may be limited. To reach the economics of scale, a "farm" of wave energy converters should be densely packed in arrays (Johanning et al., 2007). The limiting factor of how dense the arrays can be placed is determined by the mooring footprint and by how close the devices can be without interfering with one another.

Several solutions are proposed and tested in the last 5 years, such as SeaFlex (Seaflex, 2020), Tfi mooring tether (Tfi, 2012), and Exeter tether (Gordelier et al., 2015). They aim to tackle the contradicting engineering challenge required by WEC mooring systems. A tether component, in the mooring context, is a mechanical system designed to reduce mooring and anchor loads (Magagna et al., 2018). It is typically attached in series to the mooring lines, between the end of the mooring line and the anchor. An example is shown in Fig. 1-1, which is a tether component designed by SeaFlex. These developments have triggered the interest of evaluating the effects on the WEC performance, in particular the mechanical service life of the mooring system and its power performance, of elastic mooring systems with and without such tether components.

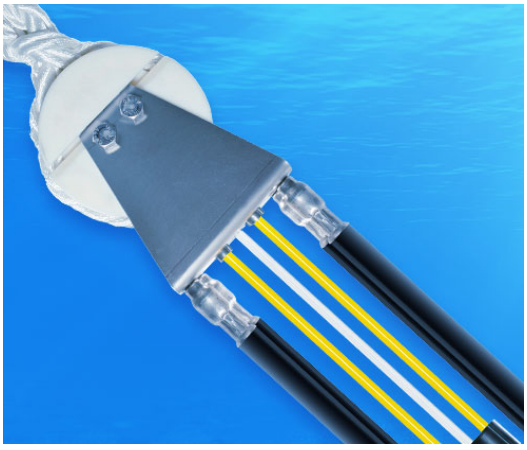

Figure 1-1: Seaflex tether component (Seaflex, 2020).

1.2 Objective and goals

The main objective of this thesis is to develop a numerical model and simulation procedures for elastic mooring systems and compare the performances of the WEC system. The numerical method is chosen rather than physical experiments because material testing can be expensive and time-consuming, as are ocean basin tests or full-scale on-site tests. Modern technology developments hence heavily rely on numerical simulation to cut down the time and money invested in physical tests. Numerical simulations also offer the possibility of studying a wide variety of parameters within a short time frame and relatively low cost. Thus, this thesis project's investigations proceed with numerical methods, i.e., mechanical behavior of tether component and the WEC system's motions under different wave loads are simulated numerically.

To achieve the objective, smaller goals are proposed to build up the steps leading to the main objective. The goals are:

1. Develop numerical models for the tether component, mimicking the non-linear, strain-rate-dependent, and load-path-dependent material behavior. Parametric sensitivity analysis is carried out.
2. Compare the impact of integrating tether component into the mooring configuration, with parametric sensitivity analysis on the environmental loads and design parameters.
3. Verify the simulations and calculations by comparing them with validated reference cases.
4. Compare the levelized cost of energy (LCoE) of elastic mooring solutions. This is a method often used in the renewable energy sector, where the assessment takes the life cycle of the product and the power production into consideration. The main contributors in the LCoE analysis for this thesis are the mechanical fatigue life of the mooring system and power absorption.

1.3 Assumptions and delimitations

This thesis is part of the ELASTMOOR project that has continued in the department for many years. For continuity reasons as well as time limitations, a specific WEC concept, WaveEL, is selected for this thesis as the reference case. The WEC concept was designed and developed by Waves4Power, a Swedish company (Waves4Power, 2020). The schematic representation of the reference concept is shown in Fig. 1-2. WaveEL is a floating-point absorber WEC, which is a type of wave-activated WEC, since the floating structure heaves up and down with the wave elevation and generates energy from the heaving motion. The dimensions of point-absorbers are relatively small comparing to the incident wavelength. Because of the small size, the wave directions are not important for these devices. It is more important that the devices are designed to resonant with the wave periods at their installed location to create maximum heaving motions.

This particular concept, especially the mooring system, has undergone extensive research and study, including comparison of mooring configuration (Ringsberg et al., 2018), comparison of simulation procedures (Yang et al., 2014; Yang et al., 2016), evaluation of the impact of biofouling (Yang et al., 2017), validation through experiments in ocean basin test and full-scale test at Runde, Norway

(Yang et al., 2018b). To focus on developing the elastic mooring system, the WEC system simulation set up for this thesis project is inherited from Yang et al. (2018b). Some of the numerical calculation parameters are adjusted along the research process for numerical convergence reasons.

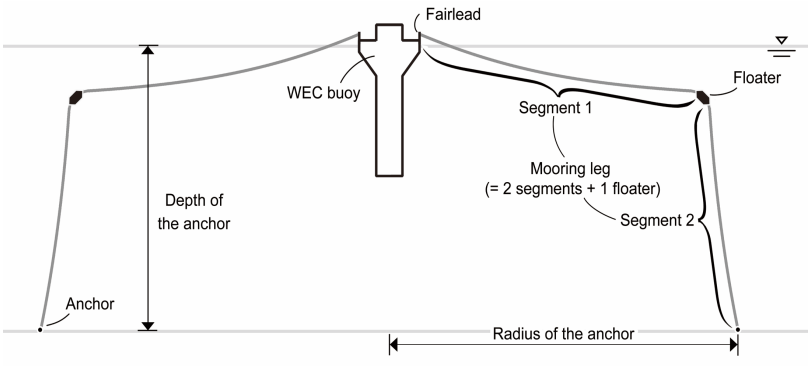

Figure 1-2: Schematic drawing of WaveEL and its mooring configuration (Yang et al., 2018).

It should be noted that although this thesis concentrates on WaveEL, a floating-point absorber WEC, the application of the elastic mooring system can be extended to different structures with similar motion characteristics.

Due to the time limit of this thesis project, several delimitations were made at the beginning of the project. As this thesis project takes WaveEL as the reference case, along with its numerical simulations setup that have been verified, most of the limitations from Yang et al. (2018b) are also inherited. The delimitations are compiled in the list below.

- PTO system: the PTO system is used for absorbing the wave energy. In this thesis, it is simplified as an ideal linear damping system. The design value of the PTO damping coefficient in heave DoF is inherited from WaveEL, which was specified by Yang et al. (2017). As the simplified PTO does not contain a control system, the power production is not optimized at each instant. This means that the power performance results are conservative.
- Material and mechanical properties of the rest of the mooring lines (i.e. the mooring lines excluding the tether component) and cables are taken as the values as they are in WaveEL, so that the comparisons are valid (Yang et al., 2018a).
- Floating WECs are typically installed in shallow water (tens to hundreds of meters), hence the effect of currents, tides, and waves are of greater significance than other offshore floating structures. However, the main motion of WEC is generated by the wave force, especially near the resonant frequency, thus the other loads are simplified and only investigated briefly to understand the different effects. The number of environmental loads is limited, only the ones that would be the most critical are simulated and compared. The details for the environmental conditions are presented in Section 3.2.2.
- Biofouling is excluded. Biofouling has been proven to have a negative impact on the WEC system on the long term (Yang et al., 2017), but since this project

is focusing on how an elastic mooring system can improve the fatigue life and power absorption performance, biofouling is excluded.

- Water depth is fixed according to each mooring configuration, which is specified in the array configuration comparison made by Ringsberg et al. (2018).
- Pretension in each mooring configuration is set with the aim of maintaining a neutral water line at device designed draft.
- The variation of wave direction is limited. The most critical wave directions are used in the simulation matrix with high priority, as it aims at design for safety. Waves from different angles are added with lower priority, for observing horizontal displacements of the WEC system. Details can be found in Section 3.2.2.
- No physical experiments are carried out in the process of this thesis. The validation and accuracy of numerical simulation relies on the research conducted by Yang et al. (2018b).
- Since this thesis is a part of the ELASTMOOR project, the damage of the mooring system is assumed to be solely on the mooring lines, and not on connecting junctions.
- As this thesis focuses on the elastic mooring systems of WECs, the power cables, the power hub and their interaction effect with the WEC and mooring system are neglected.

1.4 Outline of the thesis

The thesis is composed of seven chapters. The introduction chapter presents the identified research problem and defines the scope of this thesis project. Chapter 2 goes into detail of the theoretical background of the methods used in this project. Descriptions of the numerical simulation set up is presented in Chapter 3. Literature reviews are included in both methodology and description of numerical analysis. Chapter 4 presents selected results and findings, along with discussions on the results. Main conclusions including design suggestions, performance comparisons are presented in Chapter 5. Chapter 6 reviews the limits that were made at the beginning of the project and suggests further investigation possibilities in the future. References are listed in Chapter 7. The appendix is in Chapter 8 and holds the additional detailed information.

2 Methodology

To explore a large variety of parameter combinations in a short time frame, the investigation of improving the mooring system using elastic mooring concept focuses on using numerical methods. The numerical methods can be divided into seven categories:

1. Numerical modeling using mechanical constitutive model
2. Hydrodynamic analysis (coupled with (3), time domain)
3. Structural response analysis (coupled with (2), time domain)
4. Stress and fatigue analysis
5. Power absorption analysis
6. Parametric sensitivity analysis
7. LCoE analysis

The mechanical modeling in (1) aims to develop a constitutive model that has the desired mechanical behavior of the tether component, where it can sustain large amounts of cyclic loads, and have shock-absorption under snap loads. As the WEC buoy is elevated by the wave motions, the attached mooring lines are also moved, and vice versa. This thus requires the hydrodynamic and structural analysis be simulated together for the entire WEC system. The WEC system has sub-components linked together, and moves under the hydrodynamic forces. The hydrodynamic analysis focuses on the fluid-structure interaction whereas the structural response analysis focuses on the structure-structure coupling. Applying these two analyses to the entire WEC system, the motion and force responses can be determined for different environmental loads. The force responses of the mooring system obtained from (2) and (3) can then be processed for stress and fatigue analysis (4). The motion response of the WEC from (2) and (3) is used to predict the power absorption performance of the WEC. The fatigue analysis (4) and power analysis (5) are used for the LCoE analysis (7), where cost comparisons between the WECs with different elastic mooring systems are made. (1) can be considered as a stand-alone investigation, where the constitutive model is developed numerically using simplified cyclic strain input, and can be verified later by using the displacement response output from the coupled analysis (2) and (3), which is recommended by Flory et al. (2007). Details of the constitutive model are further described in Section 2.1.

In this chapter, the methods used in the thesis are presented and explained in detail. There are three main parts of the research, where first, the mechanical constitutive model for the tether component is built. Second, the WEC-mooring system coupled analysis is set up using SESAM package provided by DNV GL, which is specialized in coupled hydrodynamic and structure interaction (DNV GL, 2020). Lastly, the methods for post-processing of the data are described in detail. Parametric sensitivity analysis is carried out throughout this thesis project. The workflow for the research is shown in Fig. 2-1.

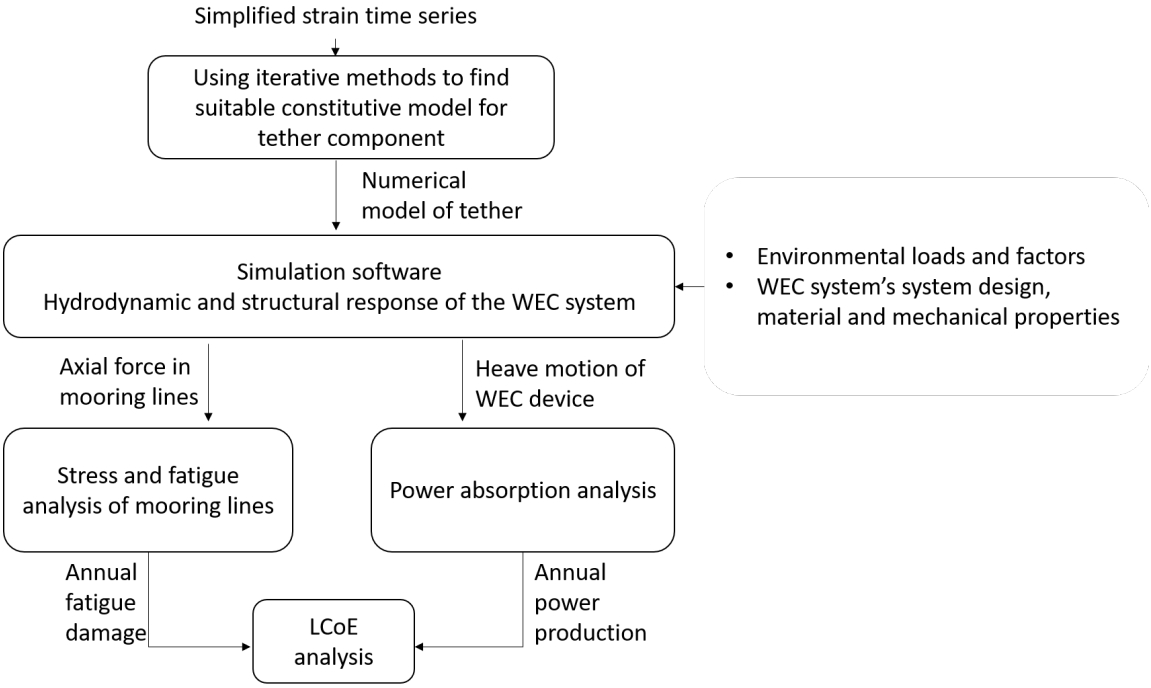

Figure 2-1: Workflow for this thesis. The boxes are the methods used in this thesis, whereas the arrows are the inputs and outputs for different analyses.

2.1 Mechanical constitutive model for tether component

Constitutive mechanical models, in the structural analysis context, describe a system's response under certain mechanical loading conditions, which provides the stress-strain relations to formulate the governing equations.

The main desirable mechanical behavior of the tether component includes the ability to sustain large cyclic loads, handling snap loads and enables large displacements without creating too much stress response, i.e. the force-strain curve should display a low axial stiffness response in operating conditions, and high stiffness in extreme, stormy conditions (Thies et al., 2014). These requirements can be translated into technical terms, that the tether component's force-strain relation should be non-linear, strain-rate dependent, and load-path dependent (Gordelier et al., 2015). Also, to prevent the mooring lines from pulling the WEC buoy down too much, thereby limiting the WEC heaving motion, the tether component should respond with only positive (tensile) stress under positive displacement. These characteristics can also be observed in the reference load-strain curve provided by Seaflex (Seaflex, 2020), see Fig. 3-1. According to Gordelier et al. (2015), the maximum limit on axial strain should also be a critical design constrain, since the tide height varies significantly in relation to the water depth. However, due to the design aim that the tether component should be applicable for different systems with different locations and water depths, the maximum axial strain is not considered as a constraint in the current status of the project.

Here, the practicality of how the constitutive model is realized with physical setup is not considered. There are, however, many solutions with similar characteristics

that were proposed by various studies: by using hydraulic cylinder (Harrold et al., 2019), reinforced rubber (Bengtsson & Ekström, 2010; Thies et al., 2014) or assembly of different rope materials (Gordelier et al., 2015; Gordeler et al., 2018). Examples such as the Exeter Tether and TFI mooring tether are presented in Fig. 2-2 and 2-3, respectively.

The intention of developing a suitable constitutive model is to investigate possible combinations of mechanical characteristics that demonstrate the desired behaviors, which can lead to more possibilities of tether development in a more efficient and cost-effective way.

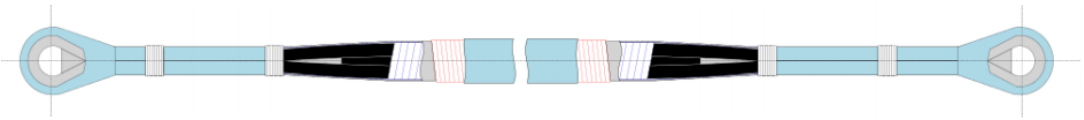

Figure 2-2: Schmatic of Exeter Tether showing the various functions along the tether: the light blue being the load carrier part, black is the elastometer core and the white/red is the anti-friction layer (Khalid et al., 2019).

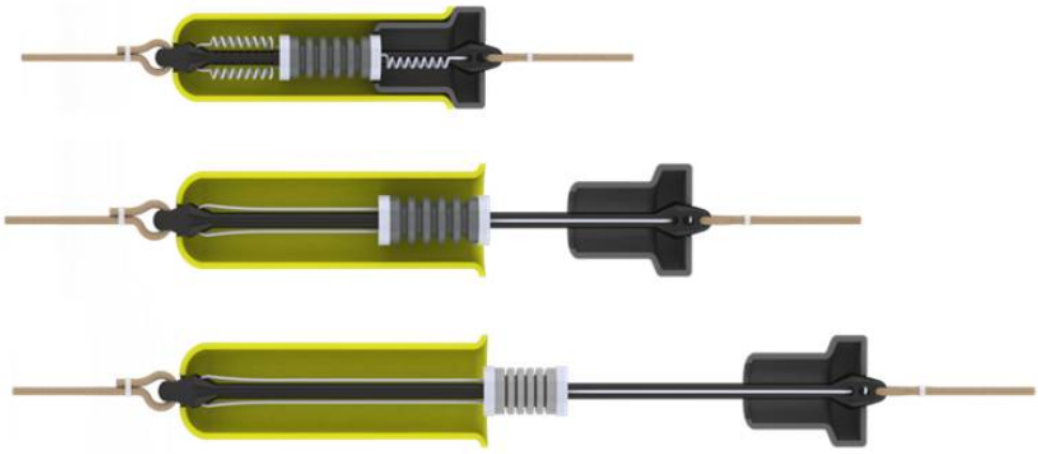

Figure 2-3: Sample image of TFI mooring tether (Tfi, 2012).

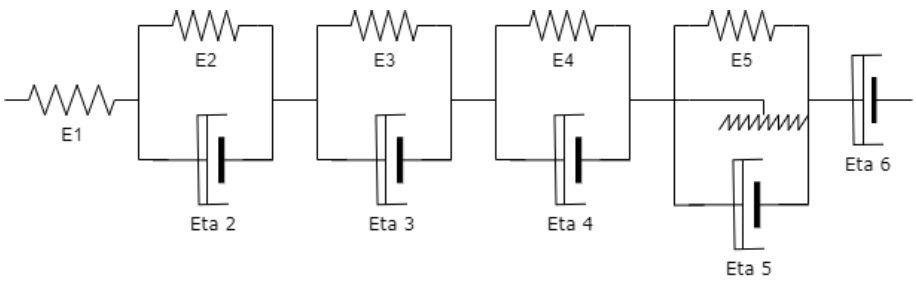

Figure 2-4: Spring-dashpot model researched by Falkenberg et al. (2019).

Various models were chosen to explore the fundamental change-in-stress response characteristics. From different literature, spring-dashpot models with 3 to 10 parameters have been investigated (Flory et al., 2007; Sebastian et al., 2008; Kim et al., 2011; Falkenberg et al., 2019). One of the most complex model among these studies was proposed by Falkenberg et al. (2019), where pairs of springs and dampers are in parallel in a series configuration, shown as Fig. 2-4. The paper concluded that the last two components were ignored, i.e., E5 and η5 were neglected due to the constructive stretch being too small, and that η6 was difficult to distinguish, and thus ignored. The other proposed models were reformulation of the basic constitutive model, which in Falkenberg's model, would be E1 the instant spring, E2 & η2 the visco-elastic spring, E5 & η5 the construction spring and η6 the creep dashpot (Flory et al., 2007; Falkenberg et al., 2019). These combinations triggered an investigation in this thesis to examine the effects of having different compositions of the spring-dashpot model, thus leading to the five basic mechanical constitutive models that are investigated. The configuration and corresponding governing equations are presented in Table 2-1.

The stress-strain relations are first compared by giving these governing equations the same strain input signal. The strain input is used to solve the ordinary differential equations (ODE) for the governing equations presented in Table 2-1. The stress responses, as solutions to the ODEs, are plotted in Fig. 2-5. An example is presented in Fig. 2-5, where all material parameters are set to 1, and the strain input is a sinus curve oscillating between 0 and 1.

It can be observed that the mechanical response from model 2 satisfies two out of three key characteristics for a desired tether: that is, it has a full hysteresis loop which provides damping for the mooring system, whilst barely having negative force response. The negative force response comes from the delayed force response caused by the damper. The slope in model 2's curve is steeper than the other models, meaning that tailoring the stiffness of model 2 to the desired value for the tether component is much more effective than the other models, which can be useful for tailoring the stiffness according to the loading condition. This observation sparked the idea of looking at the ideal load-strain curve (see Fig. 3-1) as hysteresis loops combined: one having strain values from 0 to 0.7, and another one having strain values from 0.7 to 1. If 2 basic constitutive models lay in parallel, where one part of the model only takes load under certain strain values, this may build a constitutive model that behaves similar to that is desired in Fig. 3-1.

Table 2-1: Spring-dashpot models investigated in this thesis.

Constitutive model	Governing Equation
Model1 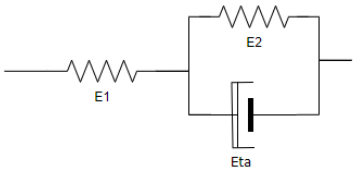	$(E_1 + E_2)\sigma + \eta\dot{\sigma} = E_1E_2\varepsilon + E_1\eta\dot{\varepsilon}$
Model2 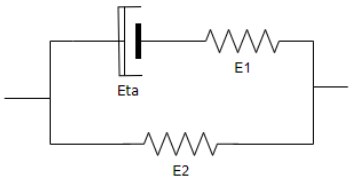	$\sigma + \frac{\eta}{E_2}\dot{\sigma} = E1\varepsilon + (\frac{E_1\eta}{E_2} + \eta)\dot{\varepsilon}$
Model3 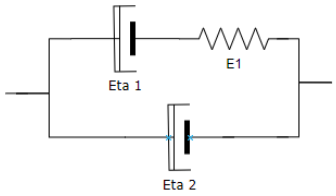	$\sigma + \frac{\eta_2}{E}\dot{\sigma} = \frac{\eta_1\eta_2}{E}\ddot{\varepsilon} + (\eta_1 + \eta_2)\dot{\varepsilon}$
Model4 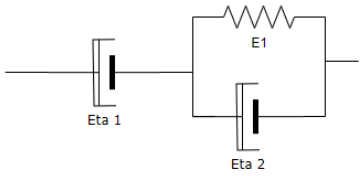	$\sigma + \left(\frac{\eta_1 + \eta_2}{E}\right)\dot{\sigma} = \eta_1\dot{\varepsilon} = \frac{\eta_1\eta_2}{E}\ddot{\varepsilon}$
Model5 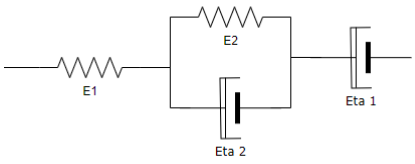	$\frac{\eta_1\eta_2}{E_1}\dddot{\sigma} + \left(\eta_1 + \eta_2 + \frac{E_2}{E_1}\eta_1\right)\ddot{\sigma} + E_2\dot{\sigma} = E_2\eta_1\ddot{\varepsilon} + \eta_1\eta_2\dddot{\varepsilon}$

Parametric studies using iterative method were carried out in order to find suitable combination of basic models to form a constitutive model that represents the desired mechanical behaviour of the tether component. The resulting constitutive model is presented in Section 4.5.

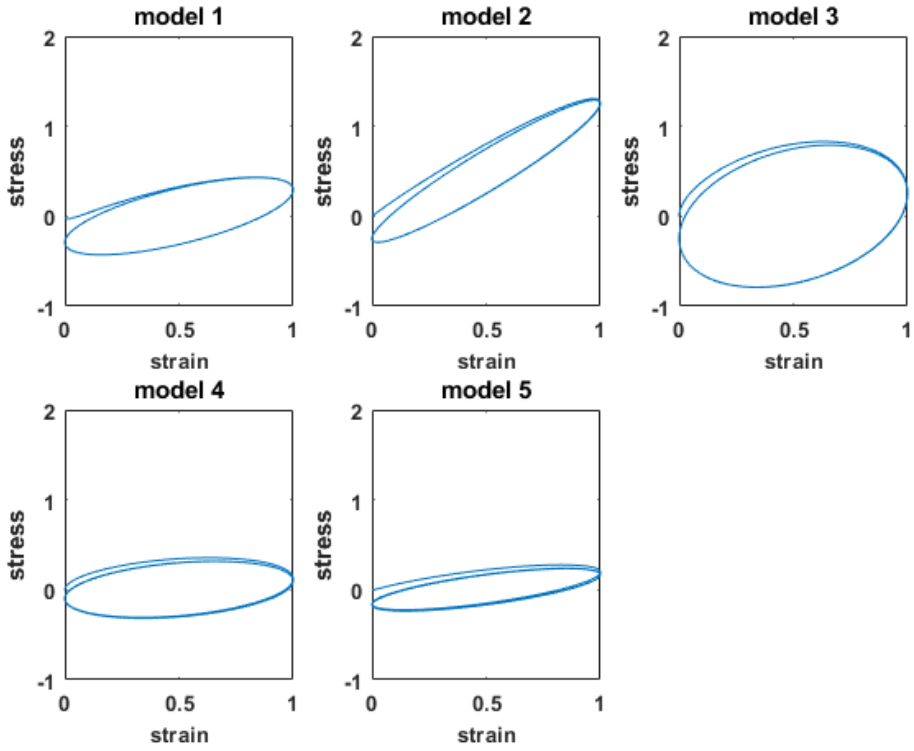

Figure 2-5: Comparison of the strain-stress relation between the 5 basic constitutive model presented in Table 2-1. All material parameters are set to 1, and the input strain is a sinus curve oscillating between 0 and 1.

2.2 Hydrodynamic and structure coupled simulations

Given that the WaveEL concept is used as the reference case in this project, the simulation procedure and modeling methods are fully adopted from Yang et al. (2018b).

Yang et al. (2016) recommend using coupled simulations as the preferred numerical methods, since it captures the interaction between the components of the WEC system better, which had been proven to be crucial for the fatigue damage calculation of the mooring lines. The word "coupled" should be clarified: there are several interaction effects in such complex simulations, such as the interaction between different components, the hydrodynamic force impacting the structures, and the structures damping the surrounding water. In this paragraph, the coupled simulation refers to the hydrodynamic and structure responses that are simulated together, so when the WEC device is excited by the wave force, it would also be affected by the mooring line motions, and vice versa. As the frequency-domain simulations cannot cope with the non-linearity in the mooring lines curvature, the time-domain coupled simulation method is selected for the computations.

Although non-linear computation fluid dynamics can capture the non-linear dynamic response of the mooring lines well, especially in the extreme loading conditions (Palm et al., 2016), the high computational expense is a huge disadvantage. The dominant hydrodynamic computation method used for simulating mooring dynamic is the potential flow theory, along with finite element

methods (FEM) (Harnois et al., 2015; Gao et al., 2016). The external wave loads are computed using the Airy wave theory, which is suitable for linear waves. The linearity of waves is defined by the wave height to the wavelength. As this thesis focuses on operational sea states with small wave heights, this approach should be sufficient for the calculation need. However, this compromise for computation expense should be kept in mind when reviewing the results.

The global WEC response is calculated for six degrees of freedom (DoF) with the boundary element method (BEM) and potential flow theory. The hydrodynamic interactions are solved considering both diffraction-induced interaction and radiation-induced interaction. The WEC buoy is simulated as a point model, where the viscous drag damping effect on the WEC device is not considered. For long cylindrical geometries, it is important to account for this effect. Morison equations are thus implemented into the simulations to account for the drag damping for both the PTO system and the WEC buoy. Mooring lines are modeled as first-order bar elements, with the hydrodynamic forces as inputs, the motion and force responses are calculated using FEM.

SESAM package provided by DNV GL (2020) is utilized for the coupled hydrodynamic-structural simulations. The solver SIMO (DNV GL, 2019d) solves for the WEC buoy's motion under environmental loads, whereas RIFLEX (DNV GL, 2019a) is another solver which deals with the mooring line structural and hydrodynamic responses. These two solvers are used through the software SIMA (DNV GL, 2019c), which provides a graphic user interface (GUI) for the easier usage. The detailed setup for the simulation can be found in Section 3.2. The corresponding core solver and its usage is summarized in Table 2-2.

Table 2-2: The sub-models, corresponding core solver and their usage that are used for the coupled hydrodynamic-structure simulations.

Sub-model	Core solver	Usage
Environmental loads model	RIFLEX & SIMO	Environmental loads acting on the WEC system
Point model of the WEC buoy	SIMO	Motion and force response of WEC buoy
Morison model of the PTO system	SIMO	Drag damping of PTO
Morison model of the WEC	SIMO	Drag damping of WEC buoy
FE model of mooring lines	RIFLEX	Motion and force response of mooring lines

2.3 Power absorption analysis

The main purpose of the WEC system is to generate electricity. For the WaveEL concept, electricity is generated through the heave movement of the WEC buoy. Once the WEC device heaving motion is obtained from the simulations, the power absorption can be calculated in terms of instantaneous absorbed wave power $P(t)$ and time-averaged wave power $\bar{P}(t)$. The equations for power calculation are shown in Eq. 2-1 and 2-2.

$$P(t) = B_{33}^{PTO}\left[\dot{\xi}(t)\right]^2 \tag{2.1}$$

$$\bar{P}(t) = \frac{1}{T}\int_0^T B_{33}^{PTO}\left[\dot{\xi}(t)\right]^2 dt \tag{2.2}$$

where ξ is the heave motion of the WEC device, and the dot represents the derivative with respect to time. T is not a fixed value, but a changing value depending on the length of the simulation. B_{33}^{PTO} is the PTO linear damping coefficient, the value used in this thesis is inherited from Yang et al. (2017) and is presented in Table 3-2.

2.4 Fatigue damage analysis

Fatigue damage happens when an object is subjected to repetitive cyclic loads. In this thesis, the axial force response in the mooring lines obtained from the hydrodynamic-structure coupled simulations are used for fatigue analysis. As the mooring lines' material response is elastic, a stress-based approach can be used. Therefore, rainflow count method (RFC) and Palmgrem-Miner cumulative rules are applicable. First, the stress response time series are processed via the rainflow count method (RFC) to obtain the stress cycles and corresponding stress ranges. Then fatigue damage was calculated based on the Palmgren-Miner cumulative rules (Dowling, 2012).

As marine energy is a relatively new sector in the energy industry, there exists only a few regulations about the WEC systems and their mooring components. According to DNV-GL, the fatigue damage for polyester mooring lines, which are the material used in the reference case, should be calculated using the relative tension instead of stress (DNV GL, 2018b). Hence, the RN (relative tension - number of cycles to failure) curve is used for the fatigue calculation. The aforementioned RFC is therefore calculated with the force response to find the force ranges. The force ranges are then transformed into relative tensions. The fatigue damage, FD, is calculated using Eq. 2.3 (DNV GL, 2018b).

$$FD = \sum_i \frac{R_i^m}{\alpha}\gamma_F \tag{2.3}$$

Here i is the i-th cycle identified using the RFC method. R_i is the ratio of the tension range to the characteristic strength, which for polyester mooring line is 95% of the minimum breaking strength (11190 kN). α and m are fatigue material properties of the polyester mooring lines and are 0.259 and 13.46, respectively (DNV GL, 2018b). γ_F is the safety factor and is recommeneded to be 60 (DNV GL, 2018b). Notice the large m and γ_F values. For materials such as steel, value for m

would fall around 3 and is around 1. This highlights two things: first, the fatigue in polyester lines are extremely sensitive to the force response range; second, though the large safety factor indicates that there is higher uncertainties due to the lack of long-term testing, it is also a result of the large *m*, where the safety factor for the relative force range is only 1.37.

2.5 Parametric sensitivity analysis

Numerous parameters would influence the power performance and fatigue life of a WEC system, such as the environmental loads, installation environment, mooring configurations, choice of mooring line material… etc. However, due to the time limit of the thesis as well as the objectives definition, the parameters investigated in this thesis are narrowed down to the mooring configuration and the environmental loads.

2.6 LCoE analysis

Levelized cost of energy (LCoE) analysis is a methodology that assesses the economical feasibility of floating offshore renewable energy farms. The method used in this thesis to LCoE is proposed by Castro-Santos et al. (2016). This method calculates the cost of the WEC development throughout the product life and takes the power production of the device into consideration. The product life is categorized into six phases, which are the concept definition, design and development, manufacturing, installation, exploitation, and dismantling. The total lifecycle cost (LCS) is the sum of the cost of these six phases. Castro-Santos et al. (2016) highlighted that the most important cost throughout the lifecycle of floating offshore renewable energy farm is the exploitation cost, manufacturing cost, and the installation cost.

The annual energy produced from the device is calculated using Eq. 2.4 (Yang et al., 2018a).

$$E = P \cdot 24 \cdot 365 \cdot \eta_{Availability} \cdot \eta_{Transmission} \tag{2.4}$$

where $\eta_{Availability}$ is the availability of the power production and $\eta_{Transmission}$ is the efficiency of transmission. The values are set as 0.95 and 0.2, respectively, which are recommended by Pecher & Kofoed (2017).

The levelized cost of energy is calculated using Eq. 2.5 (Castro-Santos et al., 2016).

$$LCoE = \frac{\sum_{n=0}^{n=N} \frac{LCS_n}{(1+r)^n}}{\sum_{n=0}^{n=N} \frac{E}{(1+r)^n}} \text{ (unit: EUR/MWh)} \tag{2.5}$$

where *N* is the designed service life in years, *LCS* is the total cost of the WEC system throughout the product life time in Euro, E is the annual energy production in MWh, *r* is the capital cost of the project. *N* is set as 25 years according to Pecher & Kofoed (2017) and and *r* is set as 1.10 according to Vance (2018).

Yang (2018) concluded that if the fatigue damage and power performance are not accounted for in the LCoE analysis, the cost is underestimated. Hence this thesis uses the resulting fatigue damage and power performance for the LCoE analysis for WEC with different elastic mooring systems. Most of the costs for exploitation, manufacturing and installation used in this thesis take reference from Vance (2018).

As the design of tether component is dependent on the specific load and application, the cost of tether is also project-specific and is determined case by case. Since the cost of tether is not determined, the calculated LCoE is not an absolute value for the WEC systems. This thesis makes a cost recommendation for tether instead. The cost recommendation is determined by the fatigue life, i.e. the frequency of mooring line replacements. The assumption is that the tether will improve the fatigue life of the mooring system, reducing the replacement frequencies and thus reduce the total cost for the WEC system. Results can be found in Section 4.6.2.

3 Numerical analysis

Chapter 3 is dedicated to the analysis using numerical methods. This includes the numerical modeling for the tether component (Section 3.1) and the coupled hydrodynamic-structure analysis in Section 3.2, which goes into details of the numerical setup and the simulation matrix.

3.1 Modeling tether component for coupled simulations

A tether component is a device that is attached in series to the mooring line, see example in Fig. 1-1. The tether component is typically soft during operation condition and stiff under extreme loads; it hardly undertakes compression. The benefit of adding a tether component to the mooring line is that due to its sensitivity to tension, the larger displacement would be mostly handled by the tether component, hence fulfilling both the requirement of giving large freedom for WEC device to heave, and to reduce the stress response in the mooring lines.

Several load-strain relation curves have been studied by Falkenberg et al. (2019) and Thies et al. (2014). For this thesis, the strain-load relation takes reference from Seaflex, where their technical report stated that the Seaflex tether product behaves as the load-strain curve shown in Fig. 3-1 (Seaflex, 2020). This load-strain curve is set as the aim for how the numerical model developed in this thesis should behave.

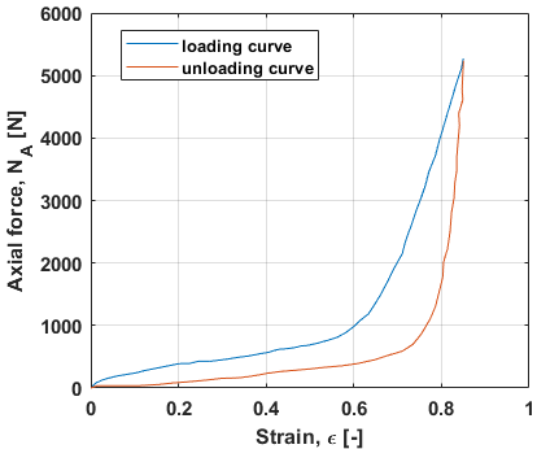

Figure 3-1: Force-strain relation of Seaflex tether component. This is taken as a reference for the desired behavior of the tether component (Seaflex, 2020).

As the aim of the thesis is to compare elastic mooring solutions, it is of interest to compare mooring setups with and without tether components, i.e., incorporating tether components in the mooring systems for the coupled hydrodynamic-structural simulations. To implement a tether component into the mooring system in the coupled hydrodynamic-structural simulations in SIMA (DNV GL, 2019c), the tether component can be modeled as a shorter line component with specified stiffness and damping, which is attached between the end of the mooring line and the anchor, see Fig. 3-2 and 3-3 for the schematic drawings. The axial stiffness can be assigned to be nonlinear with damping.

Since the development for the tether component's constitutive model takes an iterative method to find suitable material parameters, it was not ready to be implemented when coupled hydrodynamic-structure simulations were to be carried out. To proceed with comparing elastic mooring systems with and without tethers, a tether model, tether1, which encompasses the ideal load-strain relation is implemented into the coupled hydrodynamic-structure simulation. Tether1 is modeled as a 1 meter line with two segments in series. To ensure the total length of the mooring lines remain the same, the mooring lines with tether component attached is set to be 1 meter less than the non-tethered ones.

Table 3-1. Axial stiffness for tether1, interpolated from the middle values between the loading curve and the unloading curve of the Seaflex tether, presented in Fig. 3-1 (Seaflex, 2020).

strain [-]	force [N]
0	0
0.1	136.3636
0.2	245.4545
0.3	300
0.4	409.0909
0.5	518.1818
0.6	668.1818
0.7	1309.1
0.8	2836.36

Both segments in tether1 have the same non-linear stiffness, which was the values interpolated through the mid values between the loading curve and the unloading curve in the force-strain relation provided by SeaFlex (Seaflex, 2020), see Table 3-1. The hysteresis in Fig. 3-1 is created by adding damping to the component, which is assigned to only one of the segments. The damping is set as constant, with the coefficient (C) as 100 Ns^2/m^2 and the strain velocity exponent (P) as 2 [-]. The damping force is calculated using Eq. 3.1, according to the user manual from RIFLEX (DNV GL, 2019b).

$$F = C(\varepsilon) * |\dot{\varepsilon}|^P * sign(\dot{\varepsilon}) \tag{3.1}$$

where F is the damping force, C is the damping coefficient that is strain dependent, ε is the relative elongation, and $\dot{\varepsilon}$ is the strain velocity. The values of strain velocity component P as well as damping constant C should be varied systematically to evaluate the absorption ability under extreme loads.

The result of the tether's constitutive model is presented in Section 4.5. If the resulting constitutive model with clearly defined parameters is implemented for the hydrodynamic-structural simulations, the motions and force responses of the system should ideally be similar to the current approach.

3.2 Hydrodynamic-structural coupled simulations

This section presents the simulation setup for the hydrodynamic-structural coupled simulations. Details of the mooring design, simulation setups, and simulation matrices are described.

3.2.1 Mooring designs

The particular mooring setup of WaveEL was introduced to allow the WEC device to heave freely. The concept had been verified by Yang et al. (2018b), where numerical simulations for the coupled hydrodynamic and structural response of the WEC system are validated against experiments carried out in ocean basin laboratory and full-scale testing, which was tested in Runde (Norway) between 2016 and 2018.

Thorough evaluations on fatigue life of mooring system (Yang et al., 2016), mechanical life of power cables (Kuznecovs et al., 2019), the influence of biofouling on mooring lines and power cables (Yang et al., 2017), interaction effects of array configurations (Yang et al., 2018a) of this concept have been investigated. Severe sea states with significant wave height above 6.5m have an occurrence of 8% at Runde, according to the wave scatter diagram (see Appendix 8.1, provided by Waves4Power). With the water depth of 75m at Runde, the mooring system must take large tension loads as well as be able to extend. As Dowling (2012) has stated, oscillations with large amplitudes raises the fatigue damage to the material, reducing the fatigue life and makes the system more vulnerable to sudden loads. However, material such as rubber, is able to handle elongations up to 100% of its length without compromising on the fatigue resistance ability (Thies et al., 2014).

Two mooring designs are investigated in this thesis: they are referred to as 3-leg case and 2-leg case, see Fig. 3-2 and 3-3, respectively. The 3-leg case simulation had been verified and acts as the reference case in this thesis. The floaters attached in the 3-leg case have successfully reduced the impact of the snap loads and reduced fatigue damage in the mooring system, which suggests that the stress-reduction may not be the main focus of simulations. Rather, the importance of simulating the 3-leg case is to verify the simulation procedure, which is presented by Yang et al. (2018b).

The other mooring configuration is the 2-leg-taut mooring system (later referred to as the 2-leg case), see Fig. 3-3 and 3-5. The 2-leg mooring setup is desireable for the investors because of the small mooring footprint: the mooring footprint for 2-leg case is 33% of the size for the 3-leg setup. However, Ringsberg et al. (2018) found that the 2-leg configuration has higher stress response range in the mooring lines, making the mooring system more prone to fatigue damage. As tether components aim to reduce the force response in the mooring lines, this configuration is used to compare how effective tether components are in reducing the force response, ensuring the mooring system not fail due to fatigue.

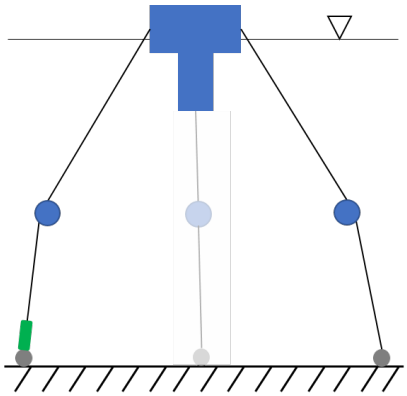

Figure 3-2: 3-leg mooring configuration, including the WEC in the upper middle, the mooring lines, the submerged floaters connecting the mooring lines and the anchors to keep the system down. The green block on the mooring line indicates where the tether component is attached in the system.

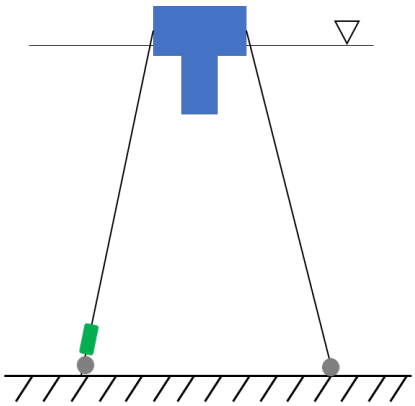

Figure 3-3: The 2-leg mooring configuration. The centerpiece is the WEC device and is moored down by 2 lines attaching to weights at the bottom. The green block on the mooring line indicates where the tether component is attached in the system.

3.2.2 Simulation model set-up

In SIMA (DNV GL, 2019c), all details of the WEC system must be specified for the simulation to run and to obtain a reasonable simulation result. The model setup is explained in detail in this section. The calculation parameters are presented in Appendix 8.3.

Water depth

As described in the mooring configuration comparison done by Ringsberg et al. (2018), the 3-leg case is simulated in 75m water depth, while the 2-leg case is simulated in 200m water depth. The 200m water depth for the 2-leg case is so that the length can give benefit to the elasticity of the mooring lines, hence it would be interesting to see if, by adding tether components, this configuration would have lower force response in the mooring lines. If this hypothesis can be proven to be true, it might open up possibilities of having the 2-leg configurations in shallower water.

Environmental loads

As the WEC system is designed to resonate with the waves, the primary focus of environmental loads is the wave forces. Regular wave conditions are simulated to see the sensitivity of WEC motion towards the wave periods. However, regular waves are unrealistic for actual operation, thus irregular waves are also investigated. Regular wave conditions are represented by wave period and wave amplitude; irregular waves are represented by the JONSWAP spectrum with 3 parameters: significant wave height (Hs), peak period (Tp), and peakedness parameter (γ).

The encounter wave directions are defined in Fig. 3-4 and 3-5, for the respected case. The conditions OP and OPc (see Table 3-4 and Section 3.2.3 for detailed

definition) have their encounter angles chosen so that the load will be parallel to one of the mooring legs, leading to this leg being subjected to constant tension. Such loading angle would be the worst case loading scenario as the other legs cannot share the tension load. One other encounter direction (i.e., condition OPd) is also investigated for the interest of horizontal displacement of the WEC device. The choice of which leg the load direction is parallel to is arbitrary, as the mooring legs in the respected mooring configuration are identical.

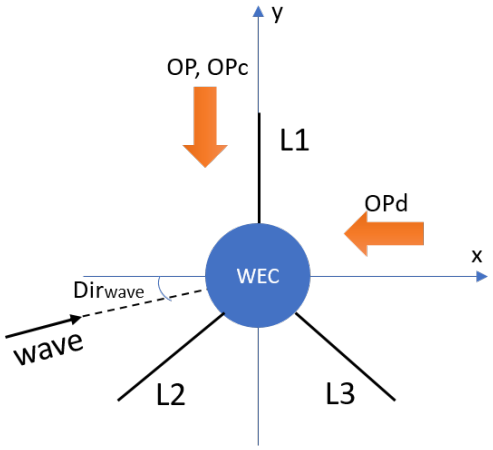

Figure 3-4: Top view of the 3-leg mooring configuration. Three legs (L1, L2 and L3) are 120 degrees apart.

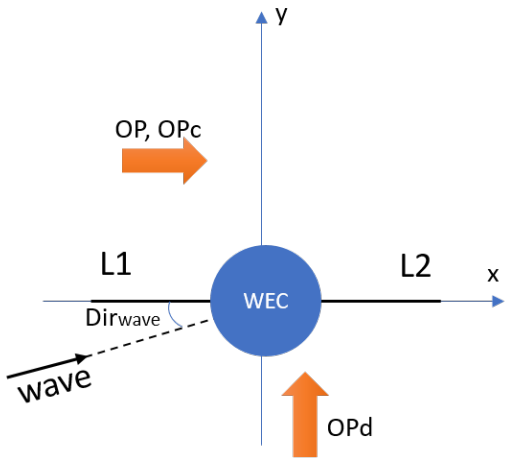

Figure 3-5: Top view of the 2-leg mooring configuration. The 2 legs (L1, L2) are 180 degrees apart.

The irregular sea states can be divided into operation sea state and severe sea state. The peak wave period falls on the natural frequency of the WEC system for the operation condition, and severe sea states are selected with large significant wave height. For the severe sea state, the effect of current and wind is taken into consideration, where sensitivity analysis is carried out by comparing the effects of computing only for severe waves and computing for complete loads. Note that as severe waves have a bigger wave height to wave length ratio, the linear waves theory that is used in this thesis may not be applicable.

Pre-tension in mooring lines

Pre-tension in the mooring lines must be set for the mooring system as the pre-tenstion affects the motion of the WEC and is WEC specific. The pre-tension determines the initial position of the WEC device, which should be at the origin point at static conditions. In this work, the configurations may have either different mooring setup (with or without tether) or different draft (200m and 75m), hence the pre-tension may vary. The correct pretension for each configuration is found via iterative process, the values are presented in Table 3-3.

Resonance period

The resonance period needs to be tested for the four cases: 3-leg with tether, 3-leg without tether, 2-leg with tether, and 2-leg without tether. This is because the resonance frequency of each system would be different depending on the model

setup. This also implies that if more than 1 tether model is simulated, different resonance periods need to be obtained.

The resonance period can be found using decay tests. It is of the essence to find the resonance period in heave direction, since this would influence the PTO performance and the fatigue damage the most.

WEC system description

The basic properties of the WEC buoy is presented in Table 3-2, the dimensions of the buoy geometry and more detailed properties are listed in the Appendix 8.2. Mooring line properties are given in Table 3-3. These values are adopted from Yang et al. (2017).

Table 3-2. Properties of WEC buoy.

Mass [kg]	2.68E+05
Draft [m]	15.265
CoG (x,y,z) [m]	(0,0,-5.247)
CoB (x,y,z) [m]	(0,0,-4.974)
PTO damping in heave DoF, B_{33}^{PTO} [kNs/m]	197.1

Table 3-3. Basic properties of mooring system for different mooring configurations.

Mooring configuration	3leg_ref	3leg_tether	2leg_ref	2leg_tether
Depth of anchor [m]	75	75	200	200
Radius of anchor [m]	145.0	145.0	47.3	47.3
Height of fairlead [m]	1.3	1.3	1.3	1.3
Pretension at fairlead [N]	13560	13560	6.17E+05	3.94E+05
Cross-section area [m^2]	0.0036	0.0036	0.0036	0.0036
Length of segment 1* [m]	96.0	96.0	194.5	194.5
Length of segment 2* [m]	64.3	64.3	-	-
Axial stiffness of each segment [N]	Nonlinear, expressed in Fig. 3-6			

*for 2-leg mooring configurations, there is only one segment in each mooring line

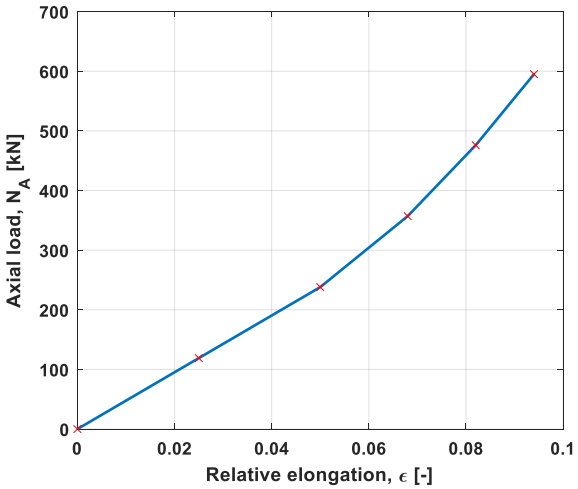

Figure 3-6: Axial stiffness of the polyester mooring described with load-elongation curve.

Coupling of WEC buoy and mooring lines

To capture the coupling effect between the WEC buoy and the mooring lines, the fairlead node of the mooring lines are modeled as a slave node to the WEC buoy, i.e., as the fairlead node of the mooring line will follow the motion of the WEC buoy.

3.2.3 Simulation matrix

As presented in Section 3.2.1, the mooring configurations can be divided into four different cases. The mooring configurations are simulated with the different environmental loads, summarized in Table 3-4. “Pre” stands for pretension tests, where the WEC device’s center of gravity (CoG) is confirmed to be at the origin point. “Decay” stands for decay test, where the WEC device is subjected to a vertical downwards force of 5000N at CoG and released, the WEC motion is then plotted along the time to find the natural period of the WEC system. Re1-3 are regular sea states simulated to observe the large motion of the WEC device in and near the resonant period. “OP” stands for operation condition and “SEV” stands for severe sea states. The subscript of the letter d indicates that the direction of loads are changed for the corresponding sea state; subscription of the letter c stands for either that current is considered, or that it is with complete load, the specifics can be found depending on the value of the wind and current velocities. The wave encounter directions for “OP” and “OPc” are chosen so that the irregular waves and currents would come from mooring leg 1, always stretching mooring leg 1 in tension. Which leg to choose is arbitrary, but by concentrating the loads on one leg, this creates the worst case loading scenario for the mooring system. As the WEC system are designed to cope with the ocean loads, it is important to assess if the system can sustain the worst loading cases. “OPd” condition is added as a parameter to verify this assumption: in 3-leg cases, the loading direction poses more tension on leg 3, whereas in 2-leg cases, the two legs should be evenly loaded, since the waves propagating direction is perpendicular to the mooring legs.

The desirable output from these simulations is the heave motion of the WEC device, which is used for power performance evaluation. The axial force responses in the mooring lines are another desired output and are used for fatigue analysis. The fatigue analysis results are compared to see whether the tether component contributes to making the fatigue life of the mooring systems at least as long as the designed service life of the WEC system.

3.2.4 Discretization of mooring lines

As the force responses in the mooring lines are solved using FEM, the mooring lines must be discretized, accordingly. The elements in the mooring line are set to be 1m long each, as this size proofs to capture the curvature of the mooring lines and gives converge computation results. This means for the 3-leg mooring cases, that there are 96 elements in segment 1 and 65 elements in segment 2; for 2-leg mooring cases, there are 145 elements in each line. Section 3.1 defines the tether component as a 1 meter segment that is attached in series to the mooring lines,

but as the tether component is relatively short comparing to the mooring lines, its discritization also needs to be finer. The element in the tether component is 0.05m long each, giving a total of 20 elements for each tether component. The count of the elements for the mooring lines start at fairlead and ends at the anchor. For the length of the mooring lines in each mooring configuration, see Table 3-3.

Table 3-4. Summary of simulated sea states.

Case name	Regular or irregular waves	Regular wave period or peak wave period [s]	Regular wave height or significant wave heights [m]	Peak enhancement parameter, γ* [-]	simulation time [s]	V_{curr} [m/s]	V_{wind} [m/s]	Dir_{wave}, Dir_{curr} and Dir_{wind}[deg]
Pre	IR	10	0.0001	1	20	-	-	0
Decay	IR	10	0.0001	1	400	-	-	0
Re1	R	0.85 T_{nat}	2	-	1200	-	-	Along L1
Re2	R	T_{nat}	2	-	1200	-	-	Along L1
Re3	R	1.15 T_{nat}	2	-	1200	-	-	Along L1
OP	IR	T_{nat}	2.5	5	10800	-	-	Along L1
OPd	IR	T_{nat}	2.5	5	10800	-	-	90 deg from L1
OPc	IR	T_{nat}	2.5	5	10800	0.514	-	Along L1
SEV	IR	8.5	7.5	5	10800	-	-	Along L1
SEVc	IR	8.5	7.5	5	10800	0.514	9	Along L1

* peak enhancement parameter describes the peak shape for the JONSWAP wave spectrum: the higher it is, the sharper the spike. The value in compliance with DNV GL (2018a).

4 Results and discussion

Sample results, along with discussion points are presented in this chapter. The results are divided into five parts: Section 4.1 presents the selected simulation results, fatigue analysis and power analysis are followed in Section 4.2 and 4.3, parametric sensitivity studies are compared and discussed in Section 4.4. Section 4.5 shows the resulting constitutive model for the tether component. Lastly, Section 4.6 presents the cost analysis results and discussion.

4.1 Coupled hydrodynamic-structural simulation results

The coupled hydrodynamic-structural simulation results presented in this thesis are mainly focused on the WEC motion and the force responses in the mooring lines.

4.1.1 Decay test

Many of the simulations in the simulation matrix presented in Section 3.2.3 aim to have the wave loads run in or near the resonant frequency of the WEC system, hence the first thing that is needed to proceed is the decay test, where resonant periods of the WEC system with different mooring setups are found through decay test.

As mentioned in Section 3.2.3, the resonant period is determined by observing the oscillation of the WEC buoy after the release of the offset force. Figure 4.1 presents the WEC motion shortly after it was being released, where the first two troughs are identified and the resonant period of the corresponding WEC system is found. The natural period of the four mooring configurations are shown in Table 4.1. Note that the different mooring cases do not differ much with respect to the natural frequency.

Table 4-1. Natural period of the WEC systems with four different mooring configurations.

Mooring configuration	Natural period [s]
3leg-ref	5.0
3leg-tether	5.0
2leg-ref	4.8
2leg-tether	4.8

Note that the 3leg-tether case (see Fig. 4.1.(b)) shows that the WEC buoy does not return to neutral water line. This is because the pretension simulations ensure the body position of the WEC is not offset by more than 0.01m, and the pretension is only adjusted if the offset is larger than 0.01m. Since the static position of the 3leg-tether case is not more than 0.01m from the waterline, the pretension of this case is not adjusted. By comparing Fig. 4.1.(c) and (d), it is visible that the tether

component has the potential to allow more heave movement in the 2-leg mooring configurations.

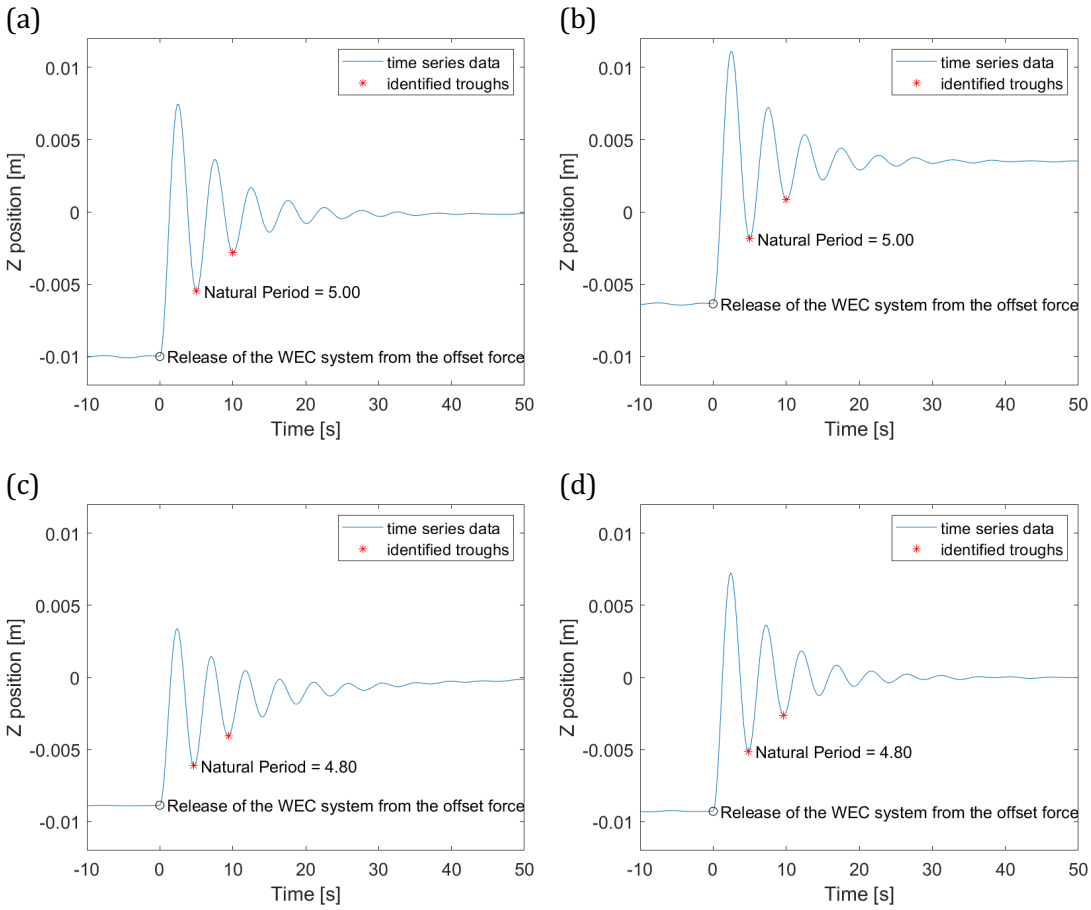

Figure 4-1: Decay test for (a)3leg-ref, (b) 3leg-tether, (c) 2leg-ref, and (d) 2leg-tether.

4.1.2 Comparison of simulated wave elevation and WEC motion

Figure 4.2 shows the relations between the wave elevations and the WEC buoy motions for the 3leg-ref case under regular wave loads (Re1-Re3), where the blue lines are the wave elevations and the orange ones are the WEC motions. The behaviors for all four mooring designs are similar when they are subjected to regular periods near or on the natural period of the WEC system: for regular wave period T= $0.85T_{nat}$, the WEC motion follows the wave elevation; for regular wave period at natural period T_{nat}, the WEC buoy resonates and thus has larger motion than the wave; for regular wave period T = $1.15*T_{nat}$, the WEC system is overexcited until it reaches its steady-state after 500 seconds, therefore the motion after 600 seconds are not included in the plots.

As the regular waves for the 3-leg cases are coming from the positive y-direction, the system is subjected to a constant wave force, which will lead to a translation of the WEC system in the y-direction. Figure 4.3 shows the WEC movements in the x and y direction for the 3leg-ref case under regular waves cases Re1-Re3. Re3 (i.e., regular waves with amplitude of waveA = 1m and period of waveT = 5.75s) shows an interesting reaction where the WEC buoy first moves along with the wave direction, but then oscillates with low frequency after steady state. This oscillation

is the second-order mooring motion, which can only be found in coupled simulation.

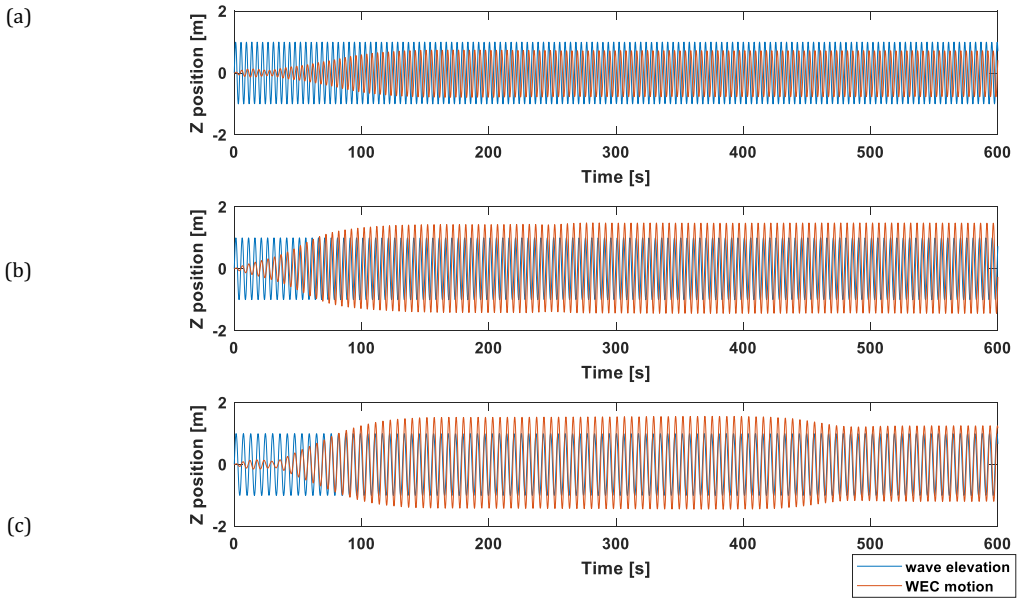

Figure 4-2: 3leg-ref case subjected to regular waves with the wave period of (a) $T = 0.85T_{nat} = 4.25s$, (b) $T = T_{nat} = 5s$, and (c) $T = 1.15T_{nat} = 5.75s$.

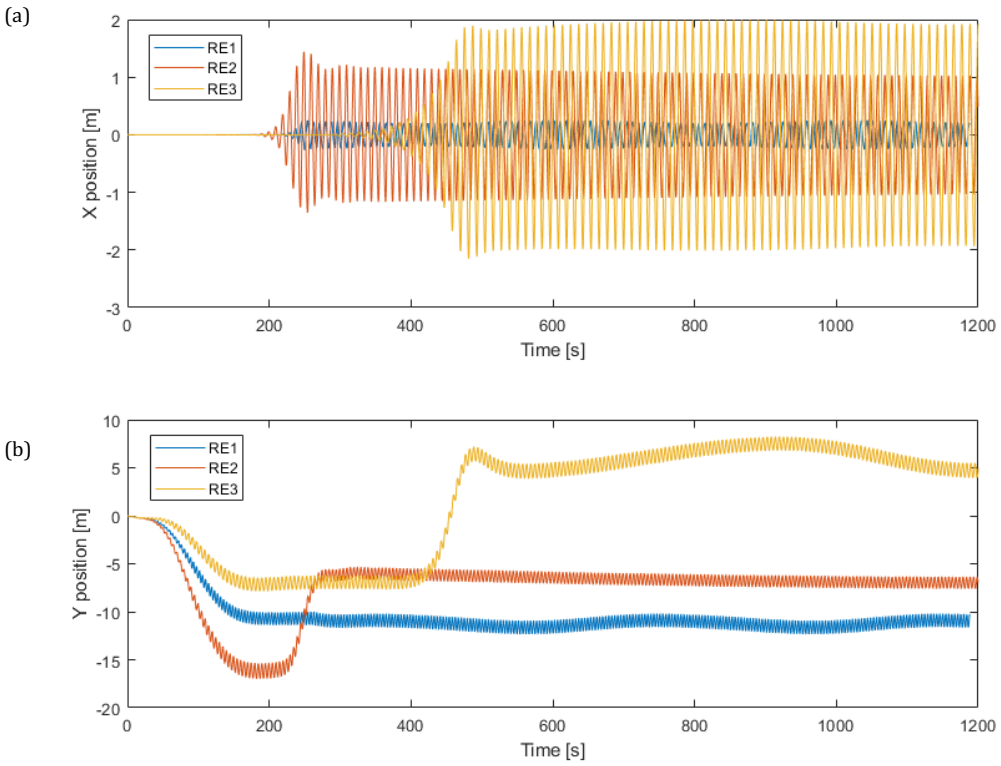

Figure 4-3: WEC motion in the (a) x and (b) y direction for the 3leg-ref case under Re1 Re2 and Re3 regular wave loads, which are T = 4.25s, T = 5s and T = 5.75s, respectively. For indication of x and y directions, refer to Fig. 3-4.

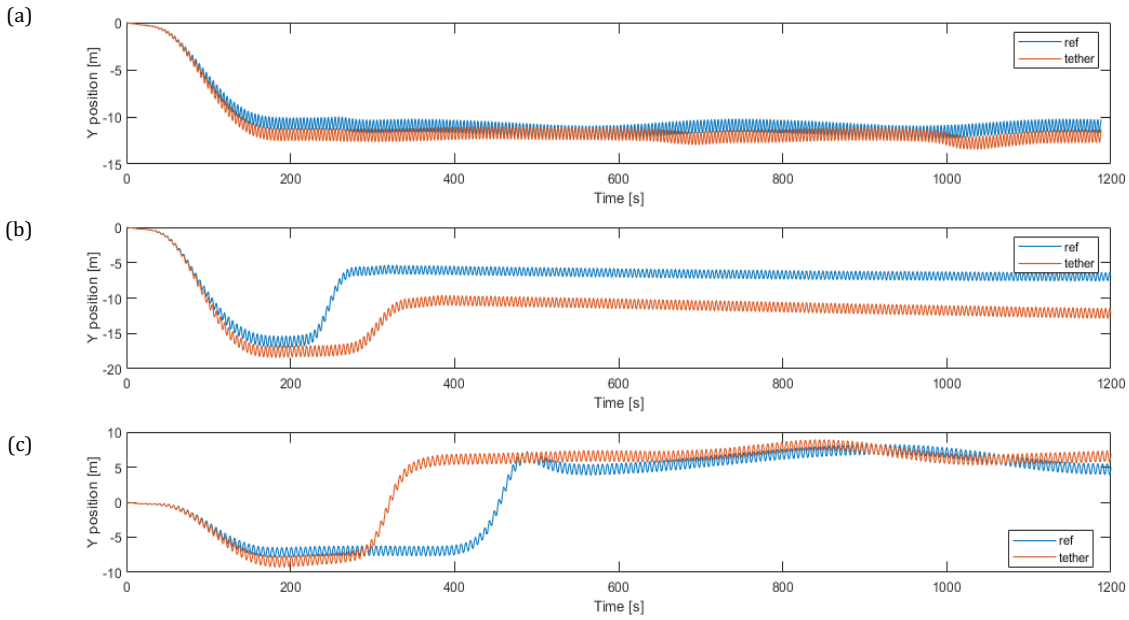

Figure 4-4: WEC motion in the y direction for the 3-leg cases under regular wave loads of (a) Re1, (b) Re2, and (c) Re3. The blue lines are the ref case and the orange ones are the tethered cases.

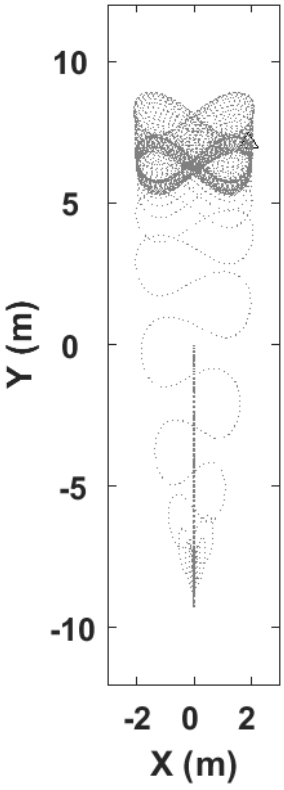

Figure 4-5: Trajectory of 3leg-tether case under Re3 regular wave case.

Figure 4-4 shows a comparison of the tethered (orange line) and reference (blue line) mooring solution reacts towards the constant wave force under different regular wave loads. A trajectory plot is presented in Fig. 4-5, where the WEC buoy starts at the origin point, oscillates in a pattern "8" until it finds its steady-state between y = 5m and y = 10m, where it forms thicker lines in the upper part of the plot.

For the 2-leg mooring solutions, the mooring lines are in parallel to the x-axis and the waves are propagating towards the positive x-direction, the constant wave force is observed in the positive x-direction, see Fig. 4-6.

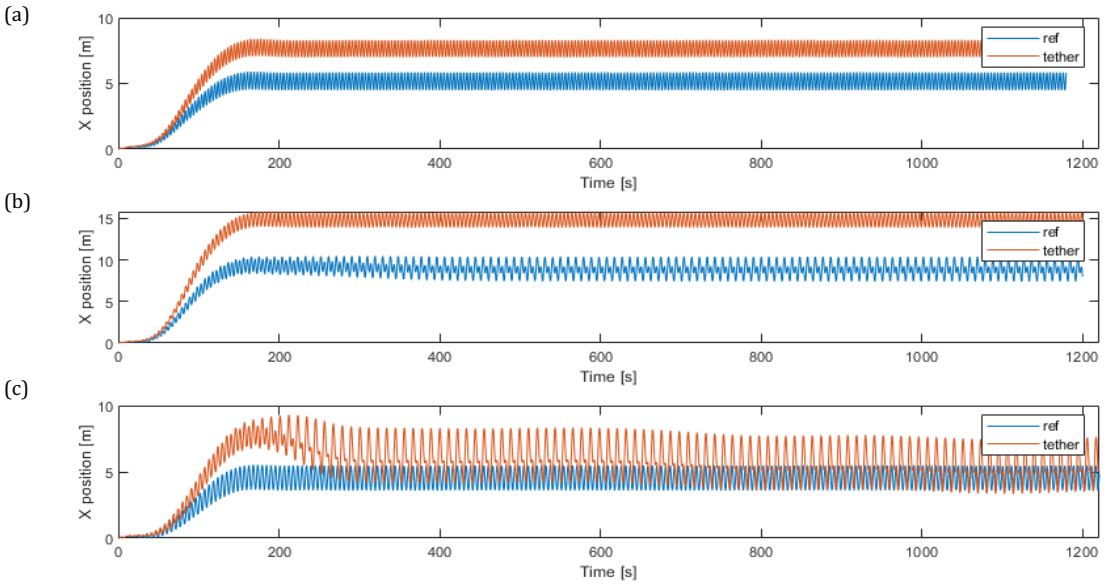

Figure 4-6: WEC motion in the x-direction for the 2-leg cases under regular wave conditions of (a) Re1, (b) Re2 and (c) Re3.

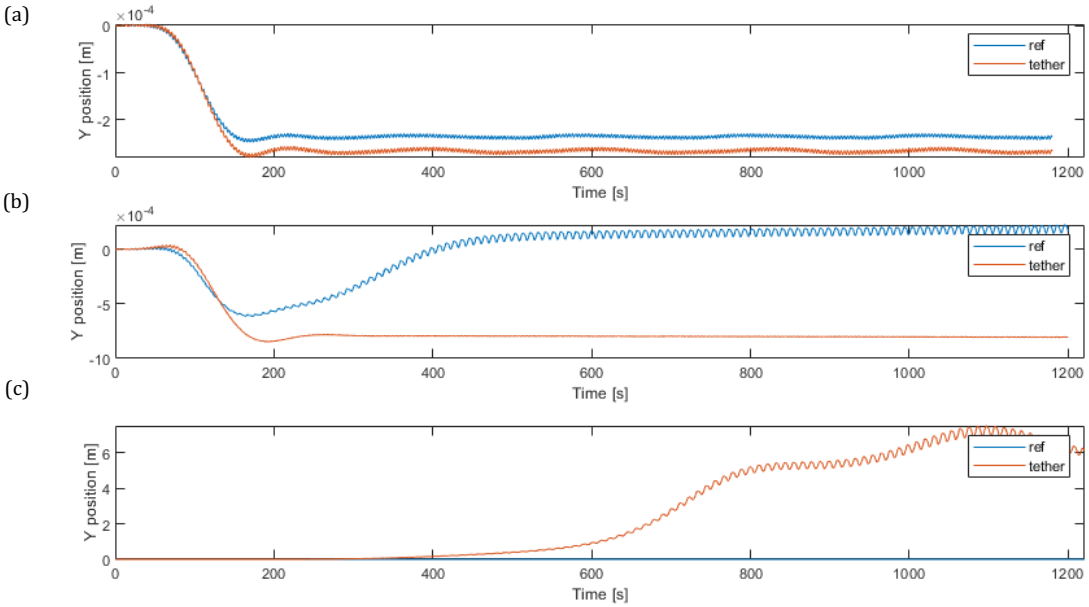

Figure 4-7: The WEC motion in the y-direction for the 2-leg cases under regular wave conditions of (a) Re1, (b) Re2, and (c) Re3.

By comparing the y-direction motion of the 2-leg WEC cases, Fig. 4-7 shows that in Re3 condition, the tethered WEC drifted perpendicular to the wave loading direction. This perpendicular drift happens as the WEC system finds its steady-state, where similar behavior can be found in Fig. 4-5 in the 3leg-tethered case. However, these drifts only happen in regular wave cases since regular waves allow the system to find steady-states, whereas, in irregular sea states, the WEC system is constantly influenced by the loading condition and rarely reaches steady-state.

In reality, wave patterns are extremely irregular and come together with wind, current and other forces, thus, the investigation of how the WEC system with

different elastic mooring system behaves continues with irregular sea state simulations.

A 3-hour time history of the heave motion of the WEC buoy under irregular condition OP (where Hs = 2.5m and Tp = natural period of the systems, respectively) is presented in Fig. 4-8. Close-ups of the WEC's heave motion of 3leg-ref case and 3leg-tether case are plotted against the wave elevation in Fig. 4-9, and the same for 2-leg cases in Fig. 4-10. It can be observed that the WEC buoy's heave motion follows the wave elevation but have a small phase difference due to the PTO damping, which agrees with the simulations done by Yang et al. (2018b).

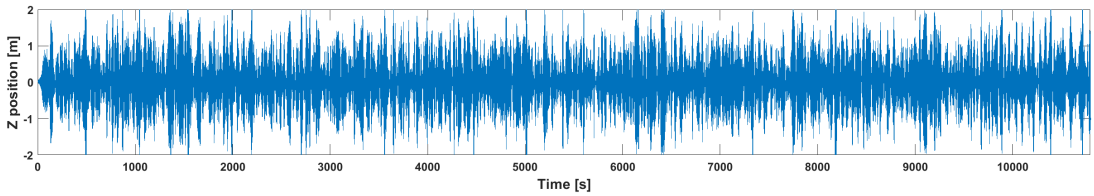

Figure 4-8: 3-hour heave motion time history of 3leg-ref case under OP condition (irregular waves only, with Hs = 2.5m, Tp = 5s, Dir_{wave} = 270 deg).

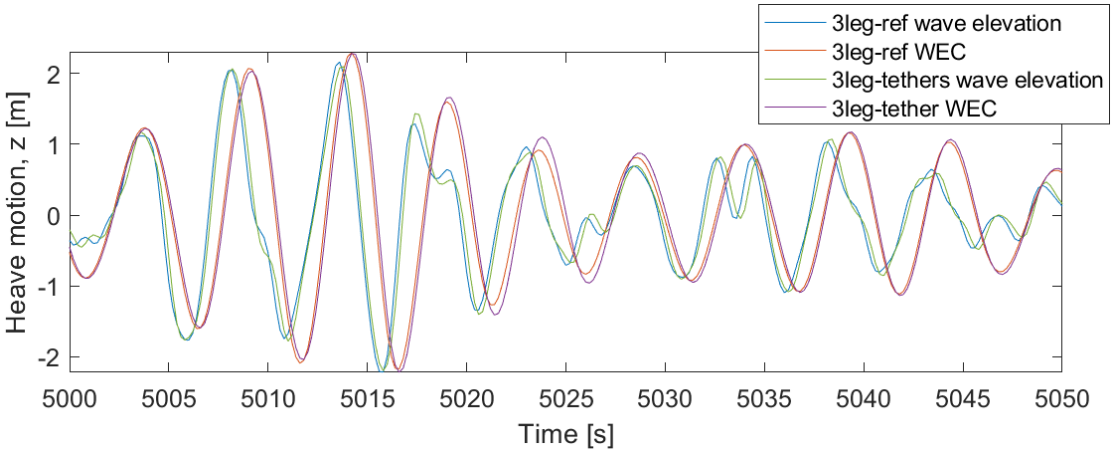

Figure 4-9: The WEC heave motion and the wave elevation for the 3leg-ref and 3leg-tether case under OP condition (irregular waves only, with Hs = 2.5m and Tp = 5s).

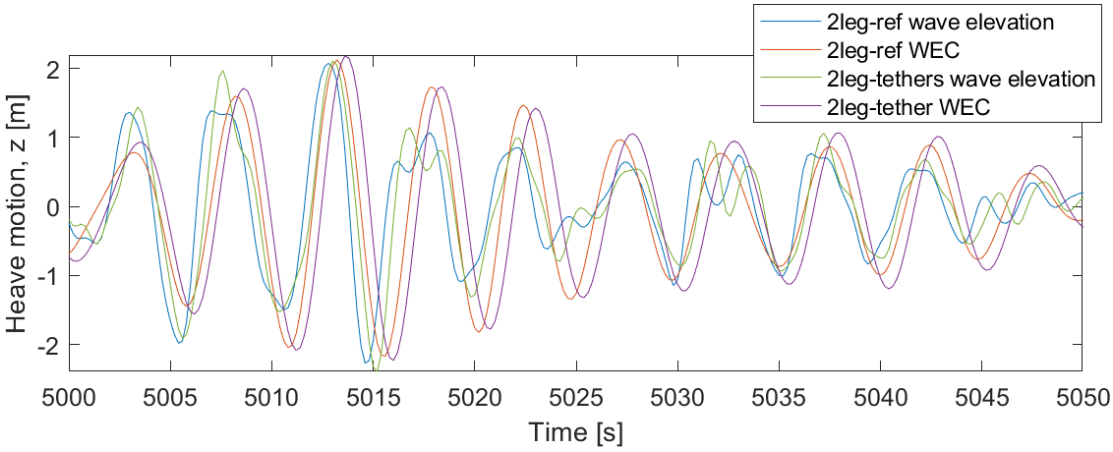

Figure 4-10: The WEC heave motion and the wave elevation for the 2leg-ref and 2leg-tether case under OP condition (irregular waves only, with Hs = 2.5m and Tp = 4.8s).

Two stable responses of the WEC buoy was found in the simulation results. First is the current force acting on the 3leg-tether case, see Fig. 4-11 (c). As the waves and current both come from positive y-direction, where L1 stands, the constant current force stabilizes the tethered WEC system and the WEC buoy does not oscillate between L2 and L3 on the x-direction; see Fig. 3-4 for direction clarifications.

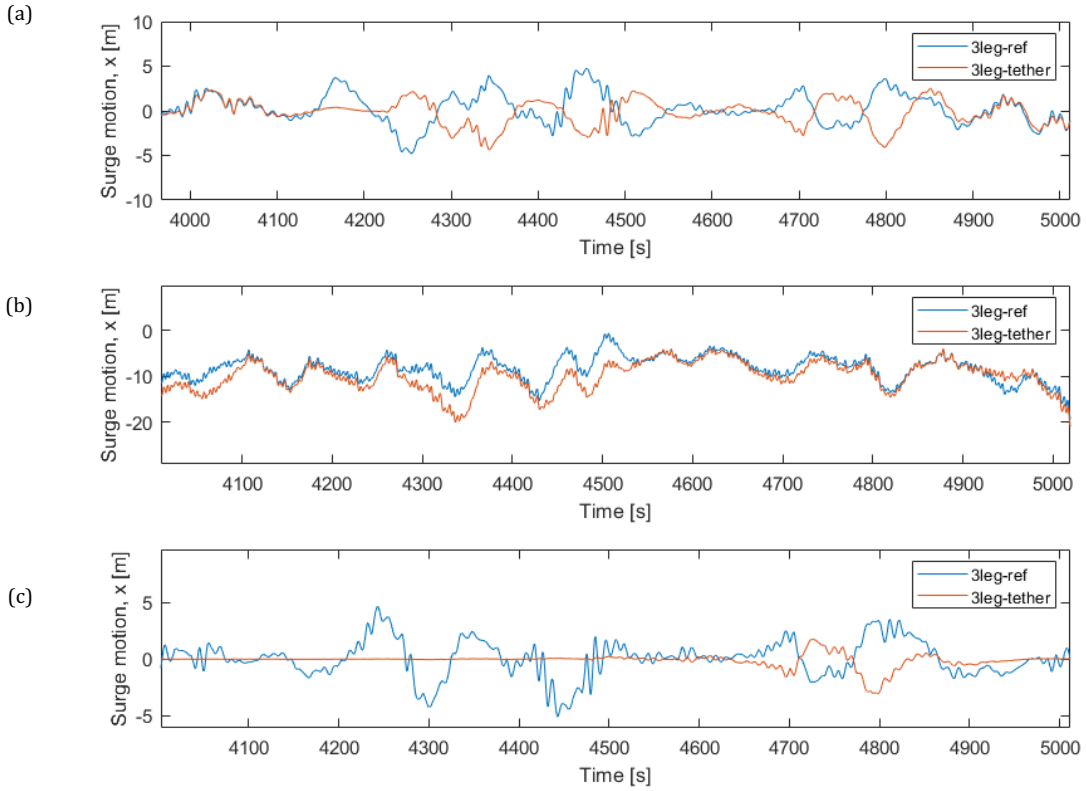

Figure 4-11: Surge motion (x direction) of the 3leg cases under operation conditions with wave parameters of Hs = 2.5m, Tp = 5 s. (a) OP: irregular waves only with Dir_{wave} = 270 deg (b) OPd: irregular waves only Dir_{wave} = 180 deg and (c) OPc: irregular waves with Dir_{wave} = 270 deg and constant current of V_{curr} = 0.514 m/s and Dir_{curr} = 270 deg.

Another stable response is the 2-leg mooring cases under wave loads that are perpendicular to the mooring lines, shown in Fig. 4-12 (b). Since the load is perpendicular to the mooring legs, it results in the two mooring legs share the load equally, therefore the buoy does not oscillate between the two legs on the x-direction. This raises the interest of investigating other encounter angles in the future for this mooring setup. For direction clarifications, see Fig. 3-5.

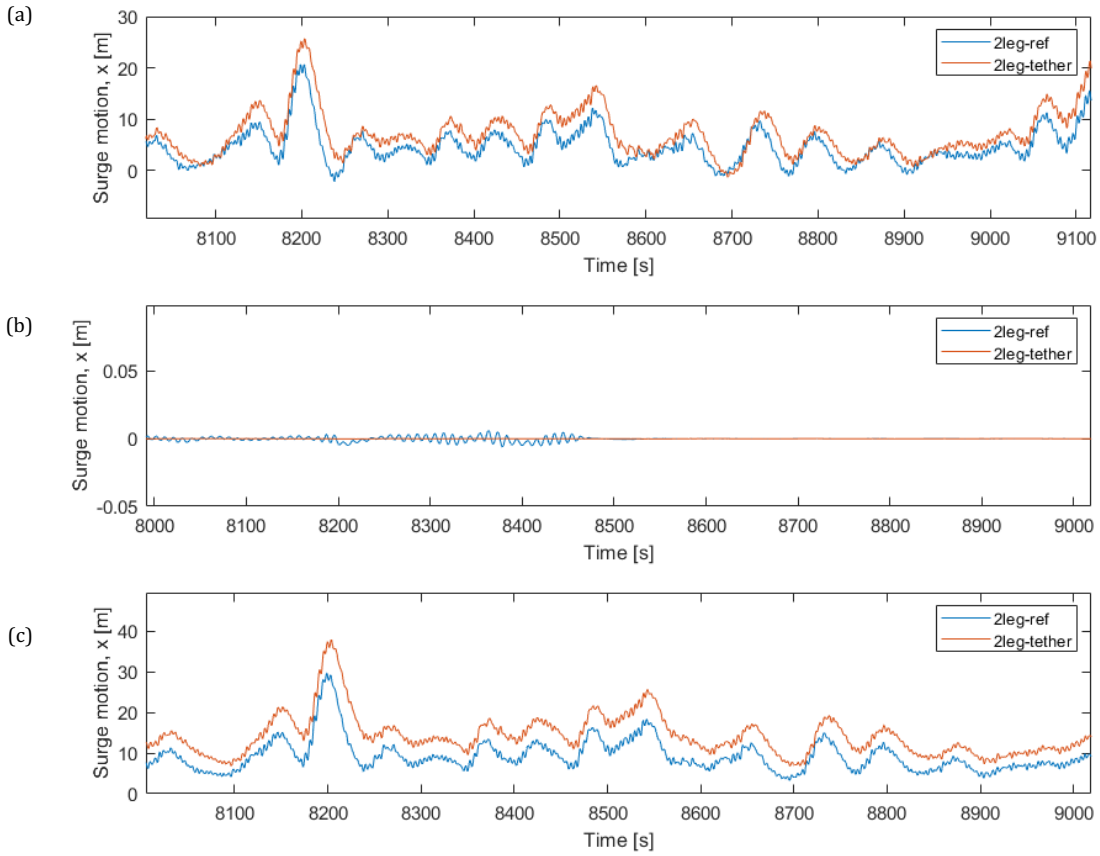

Figure 4-12: Surge motion (x direction) of the 2leg cases under operation conditions with wave parameters of Hs = 2.5m, Tp = 4.8 s. (a) OP: irregular waves only with Dir_{wave} = 0 deg (b) OPd: irregular waves only Dir_{wave} = 90 deg and (c) OPc: irregular waves with Dir_{wave} = 0 deg and constant current of V_{curr} = 0.514 m/s and Dir_{curr} = 0 deg.

Severe sea states are planned for in the simulation matrix. However, not all computations for severe conditions converged. This concurs with the remark in Section 2.2: Airy wave theory is only applicable to linear waves, which is accurate for small wave height to water depth, and small wave height to wavelength. Since severe waves have a higher wave height to wavelength ratio, Airy wave theory may not be applicable, resulting in divergence in the computation.

To summarize this section, the WEC heave motion follows the wave elevation with a small phase difference, which is useful information for both power performance and fatigue life analysis.

4.1.3 Comparison of the simulated motion and force responses in the mooring lines

This section presents the mooring lines responses under different environmental loads. A sample plot of the time histories of the axial force responses in mooring leg 1 near the fairlead is shown in Fig. 4-13. As the fairlead of the mooring line is modeled as a slave node to the WEC buoy, the force response in the mooring lines fluctuates along with the WEC motion. It can be observed that the force responses in the 3leg-tether case is slightly lower than the 3leg-ref case. Note that it is assumed that compressive loads do not contribute to the accumulated fatigue damage, hence the negative force responses are not considered in the plots.

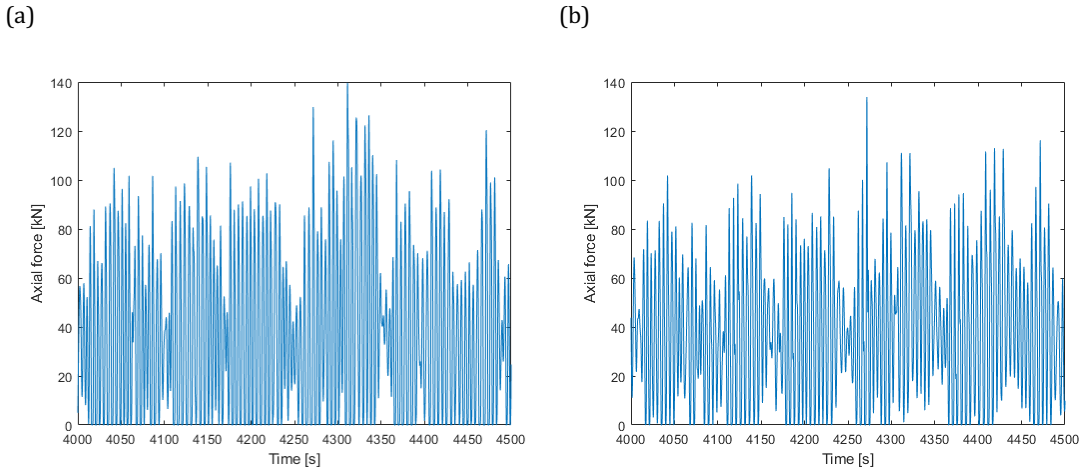

Figure 4-13: Axial force response of element #5 in leg1 for the (a)3leg-ref and (b) 3leg-tether case under OP condition (irregular waves only with Hs = 2.5m, Tp = 5s and Dir_{wave} = 270 deg).

Similar force responses can be found in the 2-leg mooring setup, as shown on Fig.4-14. Since there is no mid-buoy in the 2-leg mooring configuration acting as a damper for the system, the mean axial force in the mooring line for 2-leg mooring systems is higher by a scale of 10 comparing to the 3-leg mooring systems. It is also noticeable that the mean force is much lower for the 2leg-tether case comparing to the 2leg-ref case. This indicates that the tether component successfully reduces both the mean force response and the force responses range. As the 2leg-ref case suffers from higher stresses in the mooring lines, the tether component is more important in reducing the stress response in the mooring lines than the 3-leg cases.

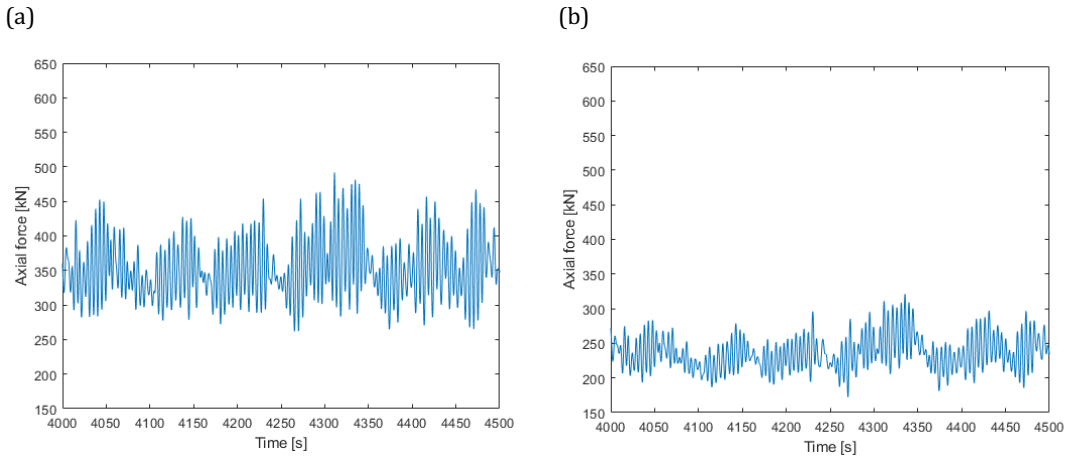

Figure 4-14: Axial force response of element #5 in leg1 for the (a) 2leg-ref and (b) 2leg-tether case under OP condition (irregular waves only with Hs = 2.5m, Tp = 4.8s and Dir_{wave} = 0 deg).

It is of vital to find the fatigue-critical location in the mooring lines, since if the weakest element fails, the whole system fails. By finding the fatigue-critical location and its fatigue life, the mechanical life of the entire system can be determined. The histograms of the force range under OP condition for a 3-hour time period are presented in Fig. 4-15 to 4-17. The windward leg in the OP condition is leg 1 and is found with a higher mean-force range, see Fig. 4-15(a) and blue bars in Fig. 4-16 and 4-17. These values are used for fatigue calculations.

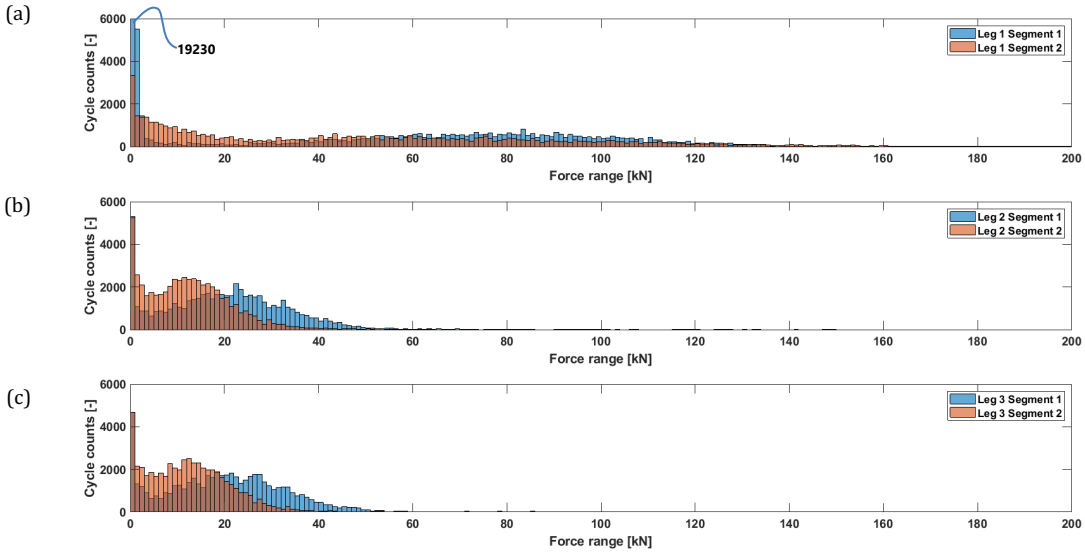

Figure 4-15: Force range for the 3leg-ref mooring case under OP condition (irregular waves only with Hs = 2.5m, Tp = 5s and Dir_{wave} = 270 deg). (a) shows the force range for leg1, (b) for leg2, and (c) for leg3.

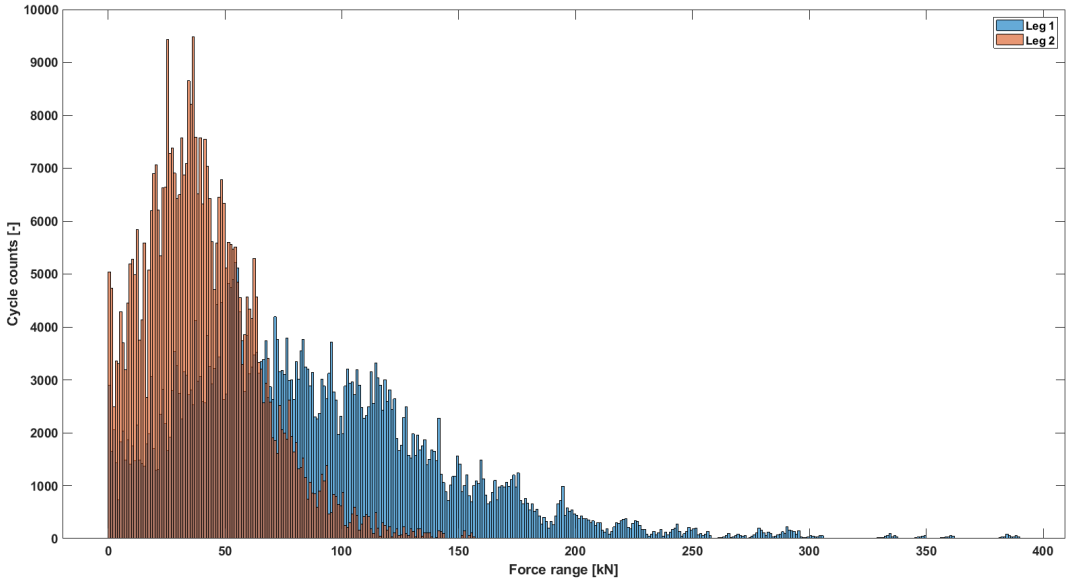

Figure 4-16: Force range for the 2leg-ref mooring case under OP condition (irregular waves only with Hs = 2.5m, Tp = 4.8s and Dir_{wave} = 0 deg).

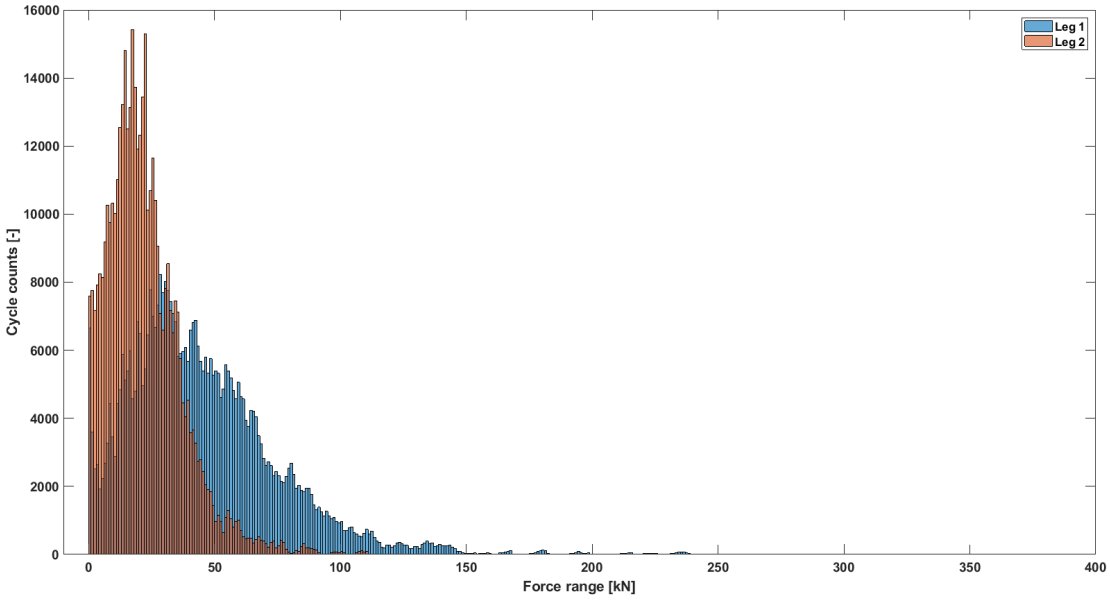

Figure 4-17: Force range for the 2leg-tether mooring case under OP condition (irregular waves only with Hs = 2.5m, Tp = 4.8s and Dir_{wave} = 0 deg).

4.2 Fatigue analysis of mooring lines

For the fatigue analysis, it should be noted that the polyester mooring ropes are modeled with no bending stiffness nor torsional stiffness, hence the calculation of the fatigue damage comes solely from the axial force response in the mooring lines. As stated in Section 4.1.3, the mooring lines do not take in compression loads, hence all negative force responses are considered 0 N. The assumption of the mooring lines not taking compressive loads reflects to how the mooring lines take slack in reality, which is a realistic assumption. However, low torsion and bending stiffness exists in the mooring lines, so by disregarding them here may lead to an optimistic fatigue life estimation.

With the force response of the mooring line obtained from the coupled hydrodynamic-structural simulations presented in Section 4.1.3., the fatigue analysis may carry on. Examples of the force response range can be found in Fig. 4-15 to 4-17. A comparison of the accumulated fatigue damage in the mooring line for a 3-hour simulation under the operational condition is presented in Fig. 4-18. Even though the fatigue damage behavior appears to be similar, the ratio between the damage for non-tethered cases to tethered cases can be 100 times or even 1000 times more, which can be observed through the different scales on the y-axis of the plots in Fig. 4-18. The reason for the large difference between the fatigue damage is due to the material parameter *m*, see Eq. 2.3. This makes the fatigue damage value extremely sensitive to the force response range, and therefore affect the fatigue life of the mooring lines significantly.

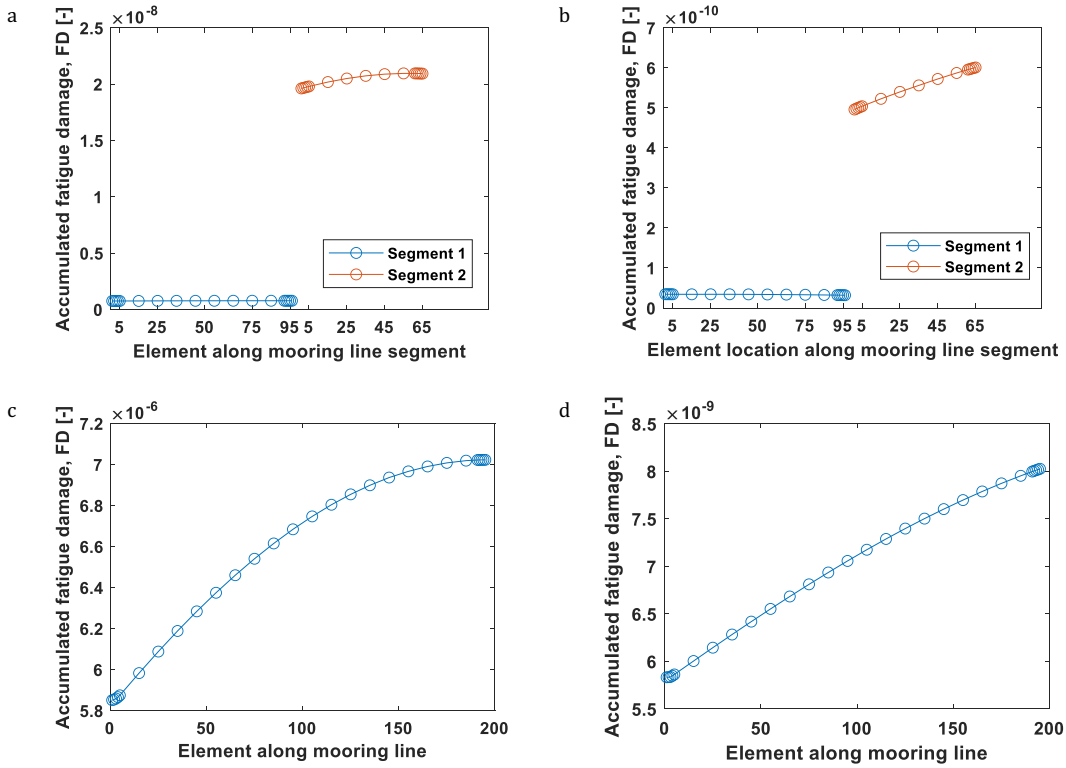

Figure 4-18: Accumulated fatigue damage along the mooring line under a 3-hour operation sea state simulation for 4 different mooring setups. The images are (a) 3leg-ref case, (b) 3leg-tether case, (c) 2leg-ref case, and (d) 2leg-tether case. Note that the scale on the y-axis is different for each plot. The element count starts from the WEC and ends at the anchor, meaning the WEC is connected at the left-hand side of these figures. The discretization is defined in Section 3.2.4, where segment 1 in 3-leg setup has 96 elements, segment 2 has 65 elements, and 195 elements for the 2-leg configuration.

If one element reaches the fatigue threshold, the whole mooring line fails. Thus, it is important to identify which element in the mooring system suffers the highest fatigue damage and the value of the fatigue damage. Fig.4-18 is an example that the fatigue damage are the highest near anchor point, but this may not be the case for all mooring configurations, nor for all sea states. For each sea state, the highest fatigue damage is used to evaluate how vulnerable the mooring system is. A comparison of the accumulated fatigue damage between the 3-leg tethered and non-tethered mooring cases under the simulated sea state is summarized as Fig.

4-19. The same comparison is made for the 2-leg cases and is presented in Fig.4-20.

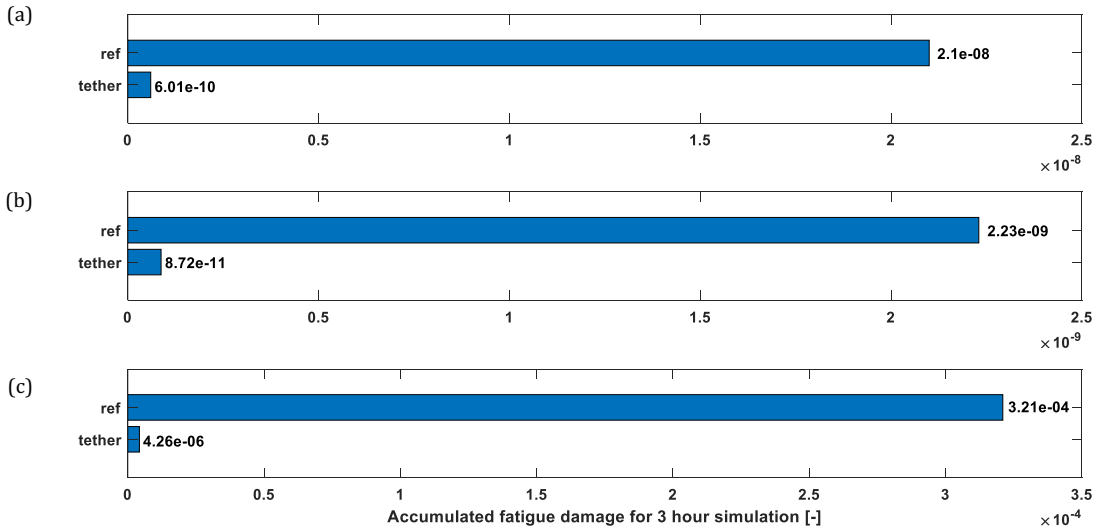

Figure 4-19: Highest accumulated fatigue damage for 3-leg mooring systems under different irregular waves sea states. All Hs = 2.5m and Tp = 5.0s, differences between sea states are: (a)OP: irregular waves only with Dir_{wave} = 270 deg (b) OPd: irregular waves only with Dir_{wave} = 180 deg, and (c) OPc: irregular waves with currents, V_{curr} = 0.514 m/s, Dir_{wave} = Dir_{curr} = 270 deg.

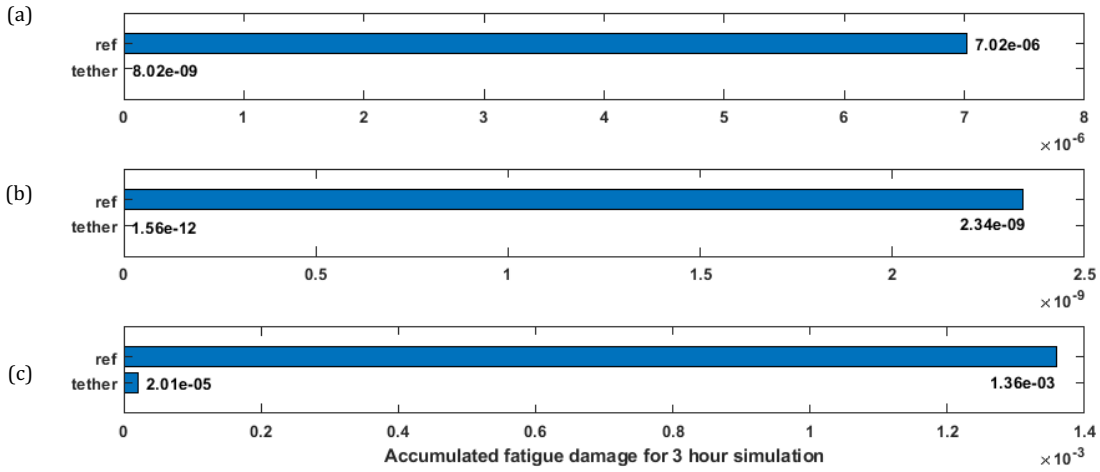

Figure 4-20: Highest accumulated fatigue damage for 2-leg mooring systems under different irregular waves sea states. All Hs = 2.5m and Tp = 4.8s, differences between sea states are: (a)OP: irregular waves only with Dir_{wave} = 0 deg (b) OPd: irregular waves only with Dir_{wave} = 90 deg, and (c) OPc: irregular waves with currents, V_{curr} = 0.514 m/s, Dir_{wave} = Dir_{curr} = 0 deg.

From Fig. 4-19 and 4-20, it is evident that the tether component reduces the fatigue damage significantly in the mooring system, under various irregular wave conditions. For all simulated cases, the fatigue damage is the highest in the windward second segment in the 3-leg mooring systems. However, the weakest element in the mooring system may differ depending on the different sea states. For the 2-leg mooring systems under OPd sea state, the waves propagating

direction is perpendicular to the mooring lines, resulting in the fatigue damage being equal on the two legs. For the fatigue damage values for each line and segment under different loading conditions, see Appendix 8.4.

With the fatigue damage value known, the fatigue life for each system under each sea state can thus be calculated and is summarized as Table 4-2. To conclude this section, the fatigue life is the shortest when the system is subjected to combined loads, especially when the direction of the loads is concentrated and comes in parallel to one of the mooring legs, see bottom row of Table 4-2. Moreover, the fatigue life of the mooring system is significantly improved by adding tether components to the system.

Table 4-2. Fatigue life for the 4 mooring cases under 3 irregular sea states. OP: irregular waves only, waves parallel to mooring leg1; OPd: irregular waves only, waves perpendicular to mooring leg1; OPc: irregular waves with current parallel to mooring leg1, V_{curr} = 0.514m/s.

	Fatigue life [years]			
Sea State	3leg-ref	3leg-tether	2leg-ref	2leg-tether
OP	$16.34*10^3$	$569.78*10^3$	48.76	$42.68*10^3$
OPd	$153.51*10^3$	$3.93*10^6$	$146.63*10^3$	$219.48*10^6$
OPc	1.07	80.48	0.25	17.07

The gray cell shows the fatigue life for the 3leg-ref case under operation condition. This value is verified Yang (2018), meaning that both the simulation procedure and fatigue calculations are correct in this thesis.

4.3 Power absorption analysis

The power absorption analysis is carried out once the WEC heave motion (see Fig. 4-8 for example) is obtained from the coupled hydrodynamic-structure simulations, which are presented in Section 4.1.2. Using Eq. 2.1 and 2.2, the instantaneous and average power absorption are calculated. The purpose of comparing the power absorbed is to know if by adding the tether component to the mooring system, the absorbed power increases or not. An example of the instantaneous power absorption and average power absorption of the 3leg-ref case under operational sea state is presented in Fig. 4-21. As the instant power absorption fluctuate greatly in every instant, only the average power absorption

is compared. A summary of the average power absorption comparison is presented in Fig. 4-22.

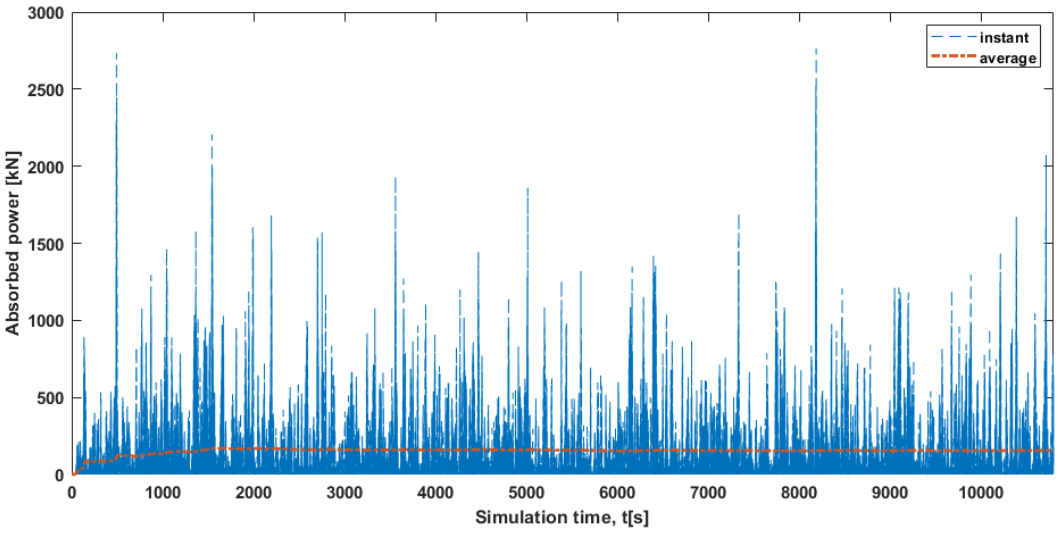

Figure 4-21: Instant and average power absorption of 3leg-ref WEC system under OP condition, where it's irregular waves only with Hs = 2.5m and Tp = 5.0s.

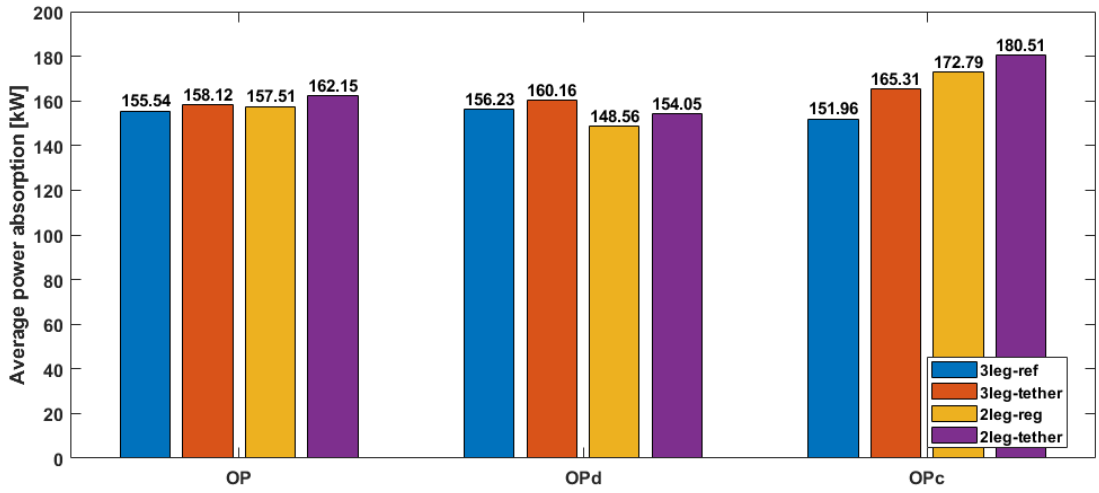

Figure 4-22: Comparison of average power absorption between the four different mooring configurations under different irregular environmental loads.

As Fig. 4-22 shows, the average power absorption differs little between mooring configurations, though the tethered setup always performs slightly better than the non-tethered case. This concludes that by adding the tether component, the power performance of the WEC system can be improved and more importantly, not negatively affected.

Note that the PTO system used in this thesis is a simplified linear damper, which behaves very different from the actual PTO system. As this linear PTO does not have a control system, the power production is not optimized for each instant. Moreover, a PTO system should protect the generator from sudden large power fluctuations, which may cause damage to the electric generator; this is also not considered in the PTO model used in this thesis project. This means that the power

production calculated in this thesis is conservative, and the actual production should perform better. Nonetheless, since all four WEC system use the same PTO model for power absorption prediction, the comparison is valid.

4.4 Parametric sensitivity analysis

The fatigue life of the 2-leg systems are always significantly shorter than the 3-legs systems under the same environmental loads, whereas the power performance of 2-leg systems are in the same range as the 3-leg systems, see Table 4-2 and Fig. 4-22. These observations align with the findings in the mooring solutions comparison presented by Ringsberg et al. (2018).

The change of loading directions of the waves, i.e., comparing OP and OPd conditions, show that the system is under the most stress if the loading is coming parallel to one of the mooring lines. The observed impact of the loading direction on the power performance of the WEC system is little.

It is of interest to see how much of an impact currents are for the WEC system's performance. As shown in Table 4-2, the fatigue life of the mooring systems under irregular waves with currents (OPc) is significantly shorter than that of without the current (OP). The constant current force creates extra tension on the mooring system, and hence reduces the fatigue life. For the 3leg-tether, 2leg-ref and 2leg-tether cases, the power performance with the current is slightly better than without the current, but the 3leg-ref case shows that the power performance is 2.3% better without the current. This concludes that the current does not have a significant impact on the power performance of the WEC system.

4.5 Constitutive model for tether component

This section presents the constitutive model for the tether component developed in this thesis. Through iterative process, it was found that by connecting two model2 in parallel and limiting one of the models to only take loads when the strain exceeds a certain value, the basic constitutive model can recreate the Seaflex force-strain relation with high similarities. The schematic spring-dashpot model is presented as Fig. 4-23 with the material parameters presented in Table 4-3. The load-strain relation with a sinus strain input is shown in Fig. 4-24.

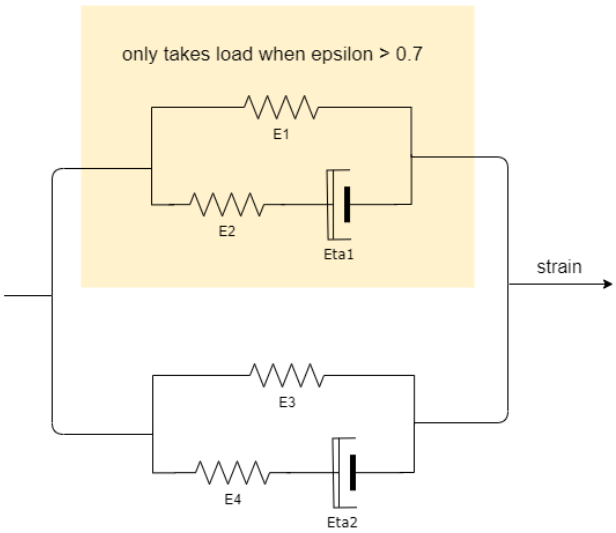

Figure 4-23: Spring-dashpot model result through iterative process for tether component.

Table 4-3. Material parameters for constitutive model for tether component.

E1 [Pa]	8e6
E2 [Pa]	8e6
eta1	0.8e6
E3 [Pa]	0.1e6
E4 [Pa]	0.02e6
eta2	2e6
Area [m2]	0.0035

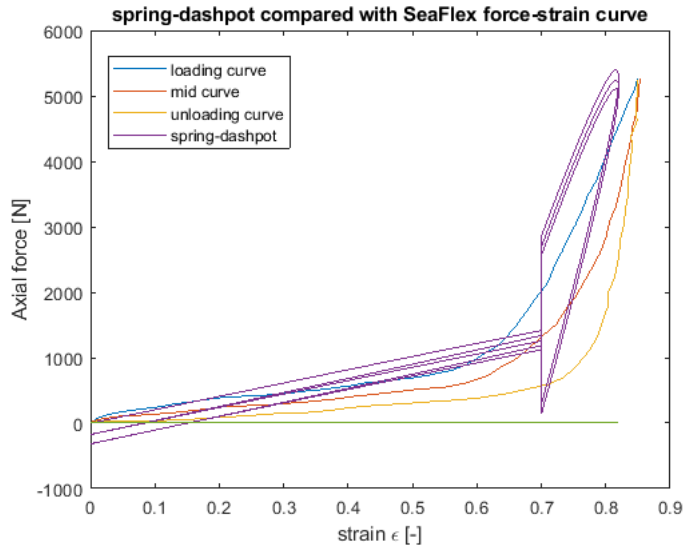

Figure 4-24: Load-strain curve comparison between the selected spring-dashpot model and Seaflex model. The purple curve is the mechanical response of the constitutive model under a strain input of a sinus wave oscillating between 0 and 1.

Although the practicality of how this model is realized in physical form is out of the scope of this thesis, the two model2 configuration can be realized using a slider connection in the tether component, so that the stiffer part of the tether would only be subjected to loading if the displacement (or strain) is too large.

SIMA (DNV GL, 2019c) offers an attractive feature, where parameters can be varied systematically. It is of importance and a possible future topic where this constitutive model is implemented into the mooring system, where coupled hydrodynamic-structural simulations are carried out with thorough sensitivity analyses on the damping coefficient (C), the strain velocity exponent (P), and the other material parameters. Due to the divergence of severe condition

computations, the current investigation does not cover the tether's snap-absorbing ability. This future investigation emphasizes on the importance of strain-rate dependency and hysteresis effects, as these are vital characteristics for snap-absorption.

Aside from varying the material parameters, it is very likely that by adding more spring-dashpot components to the constitutive model of the tether component, the load-strain curve has the potential to match the ideal mechanical behavior with closer proximity. This may lead to a mechanical component that is even more effective and efficient in reducing the axial loading in the mooring lines and absorbing the snap loads.

This constitutive model opens up two possibilities. First, this constitutive model is very different from all the literature review presented in Section 2.1. The constitutive models presented in the literatures use series connections for the basic spring-dashpot models, whereas the proposed constitutive model uses parallel connection with mechanical limitation on the model, i.e. part of the model only takes loads under certain strain ranges. This opens future possibilities in optimization for material parameters for tether component. Second, the development of constitutive model defines the necessary mechanical characteristics of a tether component, but the possibility on how to the realize it is endless.

4.6 Cost analysis

This section presents two cost analyses: LCoE analysis of different elastic mooring system and cost recommendations for tether component. As mentioned in Section 2.6, the cost of tether component is project dependent and is therefore not available for the time being. Thus the LCoE analysis would take the development, manufacture and instalment of tether component as free, assuming tether technology is in both commercially ready and competitive stage. On the contrary, the cost recommendation for the tether compares the total cost throughout the life cycle of the mooring systems, with and without tether, and the total cost difference is the maximum cost for the tether's development, manufacturing and installation.

The fatigue life and power performance that are used in the cost calculation is the OPc condition for the four mooring configurations.

4.6.1 LCoE analysis results

The levelized cost of energy for the four different mooring system is summarized as Table 4-4, including the fatigue life and power performance that are taken into account. If the fatigue life of the mooring system is lower than the designed service life, the mooring system will need replacement at some point in the product life. As shown in the first row of Table 4-4, 3leg-ref will need mooring lines replacement each year to prevent failure, and 2leg-ref case will fail within one year. For operation reasons, the mooring system would only be changed once a year, meaning for both 3leg-ref and 2leg-ref case, the mooring system will be replaced 25 times throughout the product life. The 2leg-tether case will be

replaced once during the service year, and the 3leg-tether does not require replacement throughout the product life.

The bottom two rows of Table 4-4 shows the three different considerations when calculating LCoE. LCoE1 uses recommendations from Pecher & Kofoed (2017) for the values of power availability and transmission efficiency, which are 95% and 20%, respectively. LCoE2 assumes both of these two values are 100%, according to Vance (2018).

Table 4-4. LCoE analysis for the four mooring cases. The fatigue life and power performance uses the values from OPc condition. LCoE1 assumes the power availability to be 95% and the transmission efficiency to be 20%. LCoE2 assumes 100% for both of these values.

Mooring design	3leg-ref	3leg-tether	2leg-ref	2leg-tether
Fatigue life [years]	1.07	80.48	0.25	17.07
Power absorbed [kW]	151.69	165.31	172.79	180.51
LCoE1 [EUR/MWh]	4165.1	3573.4	3150.3	2928.3
LCoE2 [EUR/MWh]	791.3	678.9	598.5	556.3

The LCoE for solar, onshore wind or offshore wind ranges from 50 to 250 EUR/MWh (REN21, 2019). Despite this analysis only considers one sea state, and that the tether component's cost is neglected, this calculation still shows that by increasing the fatigue life of the mooring system, the LCoE can be decreased. The LCoE can be significantly decreased if the transmission efficiency is improved, which is although not the focus of the thesis, still an interesting observation. Furthermore, the LCoE analysis shows that wave energy is not commercially competitive at the time being.

4.6.2 Cost recommendation for tether

The total cost for the WEC system is calculated with the six phases of product life taken into account, as suggested by Castro-Santos et al. (2016). The total cost is presented in Table 4-5, where the first row presents the total cost if all components of the mooring system (i.e., all legs, including anchors and floaters if applicable) is replaced for the maintainance, and the second row presents the total cost of only replacing one mooring leg during maintanance. The total cost for 3leg-tether case remains the same, since the fatigue life for weakest element in the mooring system is 80 years, which is much longer than the designed service life, meaning that it requires no replacement.

The total cost difference between the tethered and the non-tethered case is listed under the tethered and non-tethered total cost. This cost difference determines the maximum cost that the wave energy investors may be willing to invest in the tether instalment, which includes the research and design, manufacture, installation, and dismantling. The bottom right cell in Table 4-5 shows that 1.37

million Euro is the maximum total cost for the tether component implementation. If the tether company can develop tether technology, including the implementation, for the cost of under 1.37 million Euro, it will be more economically beneficial for the wave energy investors to install tether components. This would also be more desirable for operation reasons, since the mooring system replacement frequency can be decreased significantly with the tethers installed.

Table 4-5. Total cost for the WEC systems with four different mooring configurations.

Mooring design	3leg-ref	3leg-tether	2leg-ref	2leg-tether
Total cost, replacing all legs [EUR]	7.4707e+06	1.4572e+06	3.6630e+06	1.4930e+06
	6.01e+06		2.17e+06	
Total cost, replacing one leg [EUR]	3.8111e+06	1.4572e+06	2.7961e+06	1.4236e+06
	2.35e+06		1.37e+06	

5 Summary and conclusions

The aim of this thesis is to compare elastic mooring solutions for floating point-absorbing WEC systems on the WEC's performance, especially the fatigue life of mooring lines and the power absorption. This includes developing numerical models for tether component, simulating different elastic mooring systems under various loading conditions, verifying the calculations and simulations, and comparing the impact of different elastic mooring system on the WEC system. Finally, cost analysis is carried out to evaluate the commercial readiness of the WEC system with the elastic moorings.

Key parameters affecting the performance of a floating point-absorbing WEC were drawn from literature studies and coupled hydrodynamic-structural simulations. As the WEC system's heaving motion is dominated by the wave elevation, operation sea states with wave periods that equal to the system's resonance period were simulated. Results from the coupled hydrodynamic-structural simulations were post-processed and comparisons were made between different mooring configurations with and without tether component under various environmental loads.

A constitutive model that satisfies the desired mechanical behavior of a tether component was developed using key parameters derived from literature studies and iterative process. The proposed constitutive model has several parallel components and is unlike all the constitutive models proposed in the literature studies, which were mainly basic models in series. This opens possibilities for future investigations.

The fatigue analysis result from the reference case are compared with Yang (2018), where results were matching, verifying the simulation procedure and the calculation methods of this thesis project.

It is concluded that the tether component increases the fatigue life of the mooring system, whilst not negatively effecting the power performance of the WEC systems. These measurements are essential for the system to be economically feasible and competitive. Though the LCoE analysis is not realistic for neglecting the cost for tether and for considering only one sea state, the LCoE can be decreased by 7% to 14% through the implementation of tether. The total cost analysis suggest that the tether component will be financially more beneficial if the total cost of development, manufacturing, installation, and dismantling for the tether component for one WEC system is lower than 1.37 million Euro.

6 Future work

This chapter addresses some of the suggestions for future work. This thesis aims to investigate different elastic mooring systems for floating point-absorbing wave energy converters and their impact on the WEC system's performance, especially in the fatigue life of the mooring lines and the power performance of the WEC. The goal is to ensure longer service life for the mooring system without compromising the power performance. Design recommendations on integrating tether components into the mooring system were made. There are, however, several issues identified along the research process, that may be potential topics for future work.

Severe and survival environmental conditions

Initially, severe sea states were planned in the simulation matrix to evaluate the WEC systems performance under extreme loads. However, only one out of eight simulations converged. There are various reasons for this, firstly, the method adopted in this thesis is the usage of Airy wave theory, which only handles linear waves. Severe sea states exceed the scope of linear waves' application. The attempt of using Airy wave theory is to have an approximation of the extreme loading condition without committing to more complex simulations and higher computation expenses. That is, the assessments of severe and survival sea states require development in simulation procedures in order to accurately assess the performance of a WEC system throughout its service life.

Simulations with different installation environments

In this thesis, the mooring configurations were assigned with fixed water depth, which was the optimal value found in the mooring array configuration comparison done by Ringsberg et al. (2018). However, it was also stated that the 2-legs mooring design needs deeper water depth than the 3-leg systems to cope with the higher stresses. It would be of interest to investigate if the 2-leg mooring solution with tether components can be installed in shallower water whilst maintaining a reasonable service life.

Simulations with more environmental loads

The design of conditions OP and OPc in the simulation matrix (see Section 3.2.3.) aims to concentrate the load on one single mooring leg, which creates the most stress in the system comparing to other loading directions. However, the effects of wind, tide and stronger currents were not included in the scope of this thesis. The fatigue life calculated for condition OPc (i.e., irregular waves with currents) is significantly worse than the ones without currents (see Table 4-2), which raises the interest of simulating the mooring solution with tethers under combination

loads. Tidal change is especially of interest since it changes the water level at least twice a day and increases the stress range in the mooring lines by large.

Change of design parameters in the tether model

Section 3.1 stated that the damping coefficient and strain-velocity exponent used in the tether1 model is fixed, but these values should be varied to compare the snatch load-absorbing ability of the tether component. A more thorough sensitivity analysis on the tether component design parameter is hence a potential future topic.

Further development of the spring-dashpot model

It is evident that if more spring-dashpot components were added to the constitutive model in Section 4.5, the strain-load curve may be even closer to the ideal curve, which was used as a benchmark for how a mechanical system can help reduce the axial stress and absorb snatch loads in the mooring line. The strain-rate dependency should also be further investigated, since it is vital for the snap absorbing. Further development of the constitutive model is thus a potential future topic to investigate.

Verification of the spring-dashpot model

The current strain input for the constitutive model is a time series of sinus waves, which has changing velocities and different load paths. However, the tether should be reacting differently to varying strain velocities. Thus, the displacement time histories from the coupled hydrodynamic-structural simulations of the mooring configurations with tether components should be transformed into strain and used as the strain input for the constitutive model for a more realistic load-strain behavior.

7 References

Bengtsson, N., & Ekström, V. (2010). *Increase life cycle and decrease cost for navigation buoys.* Vinslöv: Seaflex buoy mooring systems technical report.

Castro-Santos, L., Martins, E., & Soares, C. (2016). Methodology to calculate the costs of a floating offshore renewable energy farm. *Energies, 9*(5).

Czech, B., & Bauer, P. (2012). Wave Energy Converter Concepts Design Challenges and Classification. *Ieee Industrial Electronics Magazine, 6*(2), 4-16.

DNV GL. (2018a). *DNV GL-CG-0130 Wave loads.* Høvik: DNV GL AS.

DNV GL. (2018b). *Offshore standard DNV GL-OS-E301 position mooring.* Høvik: DNV GL AS.

DNV GL. (2019a). RIFLEX V4.16-02. Høvik: DNV GL AS.

DNV GL. (2019b). *RIFLEX-user-manuel_4.16.2.*

DNV GL. (2019c). SIMA V3.7-02. Høvik: DNV GL AS.

DNV GL. (2019d). SIMO V4.16-02. Høvik: DNV GL AS.

DNV GL. (2020). *Homepage of DNV GL SESAM software*. Retrieved Febuary 1, 2020, from https://www.dnvgl.com/software/products/sesam-products.html

Dowling, N. (2012). *Mechanical behavior of materials, engineering methods for deformation, fracture and fatigue* (4th ed.). Pearson Education.

Drew, B., Plummer, A., & Sahinkaya, M. N. (2009). A review of wave energy converter technology. *Proceedings of the Institution of Mechanical Engineers Part a-Journal of Power and Energy, 223*(A8), 887-902.

EMEC. (2020). *Wave Deveopers*. Retrieved April 29, 2020, from http://www.emec.org.uk/marine-energy/wave-developers/

EuropeanCommission. (2016). *Commissioner Vella: Let's turn renewable ocean energy into a European success*. Retrieved 03 02, 2020, from https://ec.europa.eu/maritimeaffairs/content/commissioner-vella-lets-turn-renewable-ocean-energy-european-success_en

Falcao, A. (2010). Wave energy utilization: A review of the technologies. *Renewable & Sustainable Energy Reviews, 14*(3), 899-918.

Falkenberg, E., Yang, L., & Ahjem, V. (2019). Spring-dashpot simulations of polyester ropes: validation of the syrope model. Glasgow: American Society of Mechanical Engineers.

Flory, J., Åhjem, V., & Banfield, S. (2007). A new method of testing for change-in-length properties of large fiber rope deepwater mooring lines. Houston: Offshore Technology Conference.

Gao, Z., Moan, T., L., W., & Michailides, C. (2016). Comparative numerical and experimental study of two combined wind and wave energy concepts. *Journal of Ocean Engineering and Science, 1*(1), 36-51.

Gordelier, T., Parish, D., Thies, P., Weller, S., Davies, P., Le Gac, P., & Johanning, L. (2018). Assessing the performance durability of elastomeric moorings: assembly investigation enhanced by sub-component tests. *Ocean Engineering, 155*, 411-424.

Gordelier, T., Parish, D., Thies, P., & Johanning, L. (2015). A novel mooring tether for highly-dynamic offshore applications; mitigating peak and fatigue loads via selectable axial stiffness. *Journal of Marine Science and Engineering, 3*(4), 1287-1310.

Harnois, V., Weller, S., Johanning, L., Thies, P., Le Boulluec, M., Le Roux, D., . . . Ohana, J. (2015). Numerical validation for mooring systems: method and application for wave energy converters. *Renewable energy, 75*, 869-887.

Harrold, M. J., Thies, P., Newsam, D., Ferreira, C., & Johanning, L. (2019). Modeling of non-linear mooring system for floating offshore wind using a hydraulic cylinder analogy. Glasgow: American Society of Mechanical Engineers.

IEA. (2019). *World Energy Outlook 2019*. Retrieved 03 02, 2020, from https://www.iea.org/reports/world-energy-outlook-2019

Johanning, L., Smith, G., & Wolfram, J. (2007). Measurements of static and dynamic mooring line damping and their importance for floating WEC devices . *Ocean Engineering, 34*(14-15), 1918-1934.

Kempener, R., & Neumann, F. (2014). *Wave energy technology brief.* Brussels: IRENA.

Khalid, F., Arini, N., & Johanning, L. (2019). *Recommendations for WEC mooring guidelines and standards.* OPERA.

Kim, J., Kyoung, J., Sablok, A., & K., L. (2011). A nonlinear viscoelastic model for polyester mooring line analysis. Rotterdam: American Society of Mechanical Engineers.

Kuznecovs, A., Ringsberg, J., Yang, S., Johnson, E., & Anderson, A. (2019). A methodology for design and fatigue analysis of power cables for wave energy converters. *INTERNATIONAL JOURNAL OF FATIGUE, 122*, 61-71.

Magagna, D., Margheritini, L., Alessi, A., Bannon, E., Boelman, E., Bould, D., . . . L, M. (2018). *Workshop on identification of future technologies in the ocean energy sector.* Ispra: European Commission.

Magagna, D. (2019). *Ocean Energy Technology Development Report 2018.* Luxembourg: European Commission.

Palm, J., C., E., Parades, G., & Bergdahl, L. (2016). Coupled mooring analysis for floating wave energy converters using CFD: Formulation and validation. *International Journal of Marine Energy, 16*, 83-99.

Parades, G. M., Palm, J., Eskilsson, C., Bergdahl, L., & Taveira-Pinto, F. (2016). Experimental Investigation of mooring configurations for wave energy converters. *International Journal of Marine Technology, 15*, 56-67.

Pecher, A., & Kofoed, J. (2017). *Handbook of ocean wave energy.* Springer International Publishing.

REN21. (2019). *Renewables 2019 Global Status Report.* Paris.

Rinaldi, G., Thies, P., Walker, R., & Johanning, L. (2016). On the analysis of a wave energy farm with focus on maintenance operations. *Journal of marine science and engineering, 4*(3), 11.

Ringsberg, J. W., Jansson, H., Yang, S., Orgard, M., & Johnson, E. (2018). Comparison of mooring solutions and array systems for point absorbing wave energy devices. Madrid: American Society of Mechanical Engineers.

Seaflex. (2020). *Seaflex*. Retrieved 05 02, 2020, from www.seaflex.net

Sebastian, M., Unnikrishnan, K., & Narayanan, S. (2008). Viscoelastic properties of Kevlar-29 fabric tape strength member. *Mechanics of Materials , 40*(11), 949-960.

SETIS. (2013, 05 20). *Ocean Energy: Technology Information Sheet.* Retrieved 03 02, 2020, from https://setis.ec.europa.eu/related-jrc-activities/jrc-setis-reports/ocean-energy-technology-information-sheet

Tfi. (2012). *Technology from ideas: mooring tethers*. Retrieved 05 20, 2020, from https://www.technologyfromideas.com/go/technologies_for_sale/mooring_tethers

Thies, P., Johanning, L., & Mcevoy, P. (2014). A novel mooring tether for peak load mitigation: initial perfornance and service simulation testing. *Interational Journal of Marine Energy, 7*, 43-56.

TPOcean. (2017). *An Integrated Framework of Ocean Energy.* Brussels.

UN. (2020). *United Nations Sustainable Development Goals*. Retrieved May 20, 2020, from https://www.un.org/sustainabledevelopment/sustainable-development-goals/

Vance, C. (2018). *Efficient point absorbing wave energy converter configurations: influence of environment and array design.* Göteborg: Master's thesis.

Waves4Power. (2020). Retrieved 05 01, 2020, from https://www.waves4power.com/

Yang, S., Ringsberg, J., & Johnson, E. (2014). Analysis of mooring lines for wave energy converters - a comparison of de-coupled and coupled simulation procedures. San Francisco: American Society of Mechanical Engineers.

Yang, S., Ringsberg, J. H., & Palm, J. (2016). A comparison of coupled and de-coupled simulation procedures for the fatigue analysis of wave energy converter mooring lines. *Ocean Engineering, 117*, 332-345.

Yang, S., Ringsberg, J., Johnson, E., & Hu, Z. (2017). Biofouling on mooring lines and power cables used in wave energy converter systems-Analysis of fatigue life and energy performance. *APPLIED OCEAN RESEARCH, 65*, 166-177.

Yang, S.-H. (2018). *Analysis of the fatigue characteristics of mooring lines and power cables for floating wave energy converters.* Göteborg: Thesis for: Doctor of Philosophy.

Yang, S., Ringsberg, J., & Johnson, E. (2018a). Analysis of interaction effects between WECs in four types of wave farms. Lisbon: RENEW2018.

Yang, S., Ringsberg, J., Johnson, E., Hu, Z., Bergdahl, L., & Duan, F. (2018b). Experimental and numerical investigation of a taut-moored wave energy converter: A validation of simulated buoy motions. *Proceedings of the Institution of Mechanical Engineers Part M-Journal of Engineering for the Maritime Environment, 232*(1), 97-115.

Yang, S., Ringsberg, J., & Johnson, E. (2020). Wave energy converters in array configurations—Influence of interaction effects on the power performance and fatigue of mooring lines. *Ocean Engineering*.

8 Appendix

8.1 Wave scatter diagram at Runde

Table 8-1. Wave scatter diagram at the test site, Runde in Norway, the data is given by Waves4Power (Waves4Power, 2020).

Wave scatter diagram at the test side Runde in Norway (Unit: 1×10^{-5}).

H_s [m]	T_p [s] 2.5	3.5	4.5	5.5	6.5	7.5	8.5	9.5	10.5	11.5	12.5	13.5	14.5	15.5	Sum
12.5	0	0	0	0	0	0	0	1	2	3	0	0	0	0	6
11.5	0	0	0	0	0	0	0	2	7	0	0	0	0	0	9
10.5	0	0	0	0	0	0	0	11	10	0	0	0	0	0	21
9.5	0	0	0	0	0	0	6	42	10	0	0	0	0	0	58
8.5	0	0	0	0	0	2	29	87	2	0	0	0	0	0	120
7.5	0	0	0	0	0	14	107	103	2	0	0	0	0	0	226
6.5	0	0	0	0	0	44	267	33	5	1	0	0	0	0	350
5.5	0	0	0	0	7	166	337	37	7	2	0	1	0	0	557
4.5	0	0	0	0	43	558	136	32	14	5	1	1	0	0	790
3.5	0	0	0	1	371	563	123	48	19	6	2	1	0	0	1134
2.5	0	0	4	179	877	303	130	71	33	16	7	2	0	0	1622
1.5	0	0	221	1014	501	220	146	110	66	36	16	3	1	0	2334
0.5	644	367	684	248	107	142	162	192	117	64	19	22	3	4	2775
Sum	644	367	909	1442	1906	2012	1443	769	294	133	45	30	4	4	10002

Percentage: S1: 2% S2: 53% S3: 37% S4: 8%

8.2 Drawings and dimensions of WEC buoy and floaters

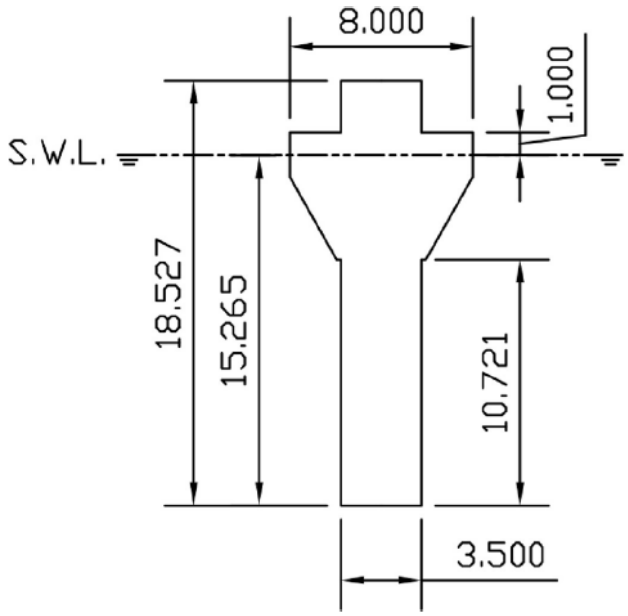

Figure 8-1: Profile view and geometrical dimensions of the WEC buoy in [m] (Yang et al., 2020)

8.3 Static and dynamic calculation parameters in SIMA for base settings

Static calculation parameters, loading sequence

No	Load type	Run with previous	N Step	Maximum iterations	Convergence norm	Accuracy
1	Volume forces	False	100	100	Displacement	1.0e-05
2	Specified forces	True	100	100	Displacement	1.0e-05
3	Specified displacements	False	100	100	Displacement	1.0e-05
4	Body forces	False	100	100	Displacement	1.0e-05
5	Current forces	False	20	100	Displacement	1.0e-05
6	Activate bottom friction forces	True	20	100	Displacement	1.0e-05

Dynamic calculation parameters

Simulation length	Time step	Requested time series length	Time increment	Wave seed	Wind seed
10800	0.005	10800	0.2	4	4

8.4 Fatigue damage - irregular sea states

3leg-ref	Leg 1				Leg 2				Leg 3				Results			
	segment 1		segment 2		segment 1		segment 2		segment 1		segment 2					
Sim#	FD [-]	weakest element	FD [-]	weakest element	FD [-]	weakest element	FD [-]	weakest element	FD [-]	weakest element	FD [-]	weakest element	weakest leg	weakest seg	Critcal FD [-]	Fatigue life [years]
OP	7.74E-10	75	2.10E-08	55	3.25E-12	15	2.28E-12	64	5.46E-13	15	3.46E-13	65	1	2	2.10E-08	1.63E+04
OPd	3.54E-11	5	4.16E-11	64	8.84E-15	15	1.44E-14	62	1.33E-10	45	2.23E-09	61	3	2	2.23E-09	1.54E+05
OPc	9.65E-05	96	3.21E-04	45	2.54E-13	2	5.56E-13	65	1.09E-12	25	2.48E-12	65	1	2	3.21E-04	1.07E+00

3leg-ref	Leg 1				Leg 2				Leg 3				Results			
	segment 1		segment 2		segment 1		segment 2		segment 1		segment 2					
Sim#	FD [-]	weakest element	FD [-]	weakest element	FD [-]	weakest element	FD [-]	weakest element	FD [-]	weakest element	FD [-]	weakest element	weakest leg	weakest seg	Critcal FD	Fatigue life
OP	3.44E-11	1	6.01E-10	65	5.65E-13	15	2.32E-14	65	1.89E-13	1	1.65E-13	65	1	2	6.01E-10	5.70E+05
OPd	2.57E-13	1	4.39E-13	65	6.26E-15	1	8.97E-16	65	1.61E-11	1	8.72E-11	65	3	2	8.72E-11	3.93E+06
OPc	1.60E-06	96	4.26E-06	65	2.12E-17	1	9.69E-18	63	2.11E-17	1	1.03E-17	65	1	2	4.26E-06	8.05E+01

2leg-ref	Leg 1		Leg 2		Results		
sim#	FD [-]	weakest element	FD [-]	weakest element	weakest leg	Critical FD [-]	Fatigue life [years]
OP	7.02E-06	195	3.89E-11	195	1	7.02E-06	4.88E+01
OPd	2.34E-09	195	2.39E-09	195	-	2.34E-09	1.47E+05
OPc	1.36E-03	195	5.40E-11	195	1	1.36E-03	2.51E-01

2leg-tether	Leg 1		Leg 2		Results		
sim#	FD [-]	weakest element	FD [-]	weakest element	weakest leg	Critical FD [-]	Fatigue life [years]
OP	8.02E-09	195	2.81E-13	195	1	8.02E-09	4.27E+04
OPd	1.56E-12	195	1.56E-12	195	-	1.56E-12	2.19E+08
OPc	2.01E-05	195	3.88E-13	195	1	2.01E-05	1.71E+01

DEPARTMENT OF MECHANICS AND MARITIME SCIENCES

DIVISION OF MARINE TECHNOLOGY

CHALMERS UNIVERSITY OF TECHNOLOGY

CHALMERS

UNIVERSITY OF TECHNOLOGY